

An extended charge-current formulation of the electromagnetic transmission problem

Johan Helsing* and Anders Karlsson†

August 29, 2019

Abstract

A boundary integral equation formulation is presented for the electromagnetic transmission problem where an incident electromagnetic wave is scattered from a bounded dielectric object. The formulation provides unique solutions for all combinations of wave numbers for which Maxwell's equations have a unique solution. This includes the challenging combination of a real positive wave number in the outer region and an imaginary wave number inside the object. The formulation, or variants thereof, is particularly suitable for numerical field evaluations as confirmed by examples involving both smooth and non-smooth objects.

1 Introduction

This work is about transmission problems. A simply connected homogeneous isotropic object is located in a homogeneous isotropic exterior region. A time harmonic incident wave, generated in the exterior region, is scattered from the object. The aim is to evaluate the fields in the interior and exterior regions.

We present boundary integral equation (BIE) formulations for the solution of the scalar Helmholtz and the electromagnetic Maxwell transmission problems. We show that our integral equations have unique solutions for all wavenumbers k_1 of the exterior domain and k_2 of the object with $0 \leq \text{Arg}(k_1), \text{Arg}(k_2) < \pi$, and for which the partial differential equation (PDE) formulations of the two problems have unique solutions. As we understand it, there is no other BIE formulation of the electromagnetic problem known to the computational electromagnetics community that can guarantee unique solutions for the wavenumber combination

$$\text{Arg}(k_1) = 0, \quad \text{Arg}(k_2) = \pi/2, \quad \text{and} \quad k_2^2/k_1^2 \neq -1. \quad (1)$$

*Centre for Mathematical Sciences, Lund University, Sweden

†Electrical and Information Technology, Lund University, Sweden

We refer to the combination (1) as the *plasmonic condition* since it enables discrete quasi-electrostatic surface plasmons in smooth, infinitesimally small, objects [25], continuous spectra of quasi-electrostatic surface plasmons in non-smooth objects [12], and undamped surface plasmon waves along planar surfaces [23, Appendix I]. Wavenumbers with $\text{Arg}(k_1) = 0$ and $\pi/4 < \text{Arg}(k_2) \leq \pi/2$ are of special interest in the areas of nano-optics and metamaterials, because in this range weakly damped surface plasmons in subwavelength objects, and weakly damped dynamic surface plasmon waves in objects of any size, can occur. These phenomena become increasingly pronounced, and useful in applications, as $\text{Arg}(k_2)$ approaches $\pi/2$ [13, 20]. It is important to have uniqueness under the plasmonic condition, despite that there are no known materials that satisfy this condition exactly, since non-uniqueness implies spurious resonances that deteriorate the accuracy of the numerical solution also for $\text{Arg}(k_1) = 0$, $\pi/4 < \text{Arg}(k_2) < \pi/2$.

It is relatively easy to find a BIE formulation of the scalar transmission problem since one has access to the fundamental solution to the scalar Helmholtz equation. It remains to make sure that the boundary conditions are satisfied and that the solution is unique. To find a BIE formulation of the electromagnetic transmission problem, based on the same fundamental solution, is harder. Apart from satisfying the boundary conditions and uniqueness one also has to make sure that the solution satisfies Maxwell's equations. Otherwise the two problems are very similar.

Our BIE formulation of the scalar transmission problem is a modification of the formulation in [15, Section 4.2]. While our formulation guarantees unique solutions under the plasmonic condition, provided that the object surface is smooth, the formulation in [15, Section 4.2] does not.

Our BIE formulation of the electromagnetic transmission problem is a further development of the classic formulation by Müller, [22, Section 23]. In [21] it is shown that the Müller formulation has unique solutions for $0 \leq \text{Arg}(k_1), \text{Arg}(k_2) < \pi/2$, but as shown in [11, Figure 9(b)], it may have spurious resonances under the plasmonic condition. The Müller formulation has four unknown scalar surface densities, related to the equivalent electric and magnetic surface current densities, and that leads to dense-mesh/low-frequency breakdown in field evaluations. Despite these shortcomings, the Müller formulation has been frequently used. Its advantages are emphasized in a recent paper [18] on scattering from axisymmetric objects where accurate solutions are obtained away from the low-frequency limit.

A modification of the Müller formulation that overcomes the low-frequency breakdown is to increase the number of unknown densities from four to six by adding the equivalent electric and magnetic surface charge densities [9, 24, 28]. The charge densities can be introduced in two ways, leading to two formulations. The first is the decoupled charge-current formulation, where the charge densities are introduced after the integral equation has been solved. The other is the coupled charge-current formulation, where

the charge densities are introduced already in the integral equations. Unfortunately, both formulations can give rise to new complications such as spurious resonances and near-resonances. Several formulations in the literature ignore these complications, but in [28] a stable formulation is presented. In line with all other formulations in literature, uniqueness in [28] is not guaranteed under the plasmonic condition.

The main result of the present work is an extended charge-current formulation of the electromagnetic transmission problem that has unique solutions also under the plasmonic condition. The road to success is to modify a coupled charge-current formulation by introducing two additional surface densities, related to electric and magnetic volume charge densities.

The formulation in [15, Section 4.2], the Müller formulation, and the formulations described in this paper are direct formulations, meaning that the surface densities are related to boundary limits of fields, or derivatives of fields. This is in contrast to indirect formulations, such as the ones in [5, 6, 16, 28], where the surface densities have no immediate physical interpretation. Our paper, and many other papers [9, 18, 21, 22, 24, 28], use integral representations of the electric and magnetic fields. It is also possible to start with representations of scalar and vector potentials and antipotentials [5, 6, 19].

The paper is organized as follows: Section 2 introduces notation and definitions common to the scalar and the electromagnetic transmission problems. The scalar problem and two closely related homogeneous problems, to be used in a uniqueness proof, are defined in Section 3. Scalar integral representations containing two surface densities are introduced in Section 4. Section 5 proposes a system of BIEs for these densities. This system contains two free parameters and, as seen in Section 6, unique solutions are guaranteed by giving them proper values. Section 7 concerns the evaluation of scalar fields. The procedure for finding BIEs for the scalar problem is then adapted to the electromagnetic problem, defined along with two auxiliary homogeneous problems in Section 8. Integral representations of electric and magnetic fields in terms of eight scalar surface densities are given in Section 9 and a corresponding system of BIEs is proposed in Section 10. This BIE system contains four free parameters and again, as shown in Section 11, unique solutions are guaranteed by choosing them properly. Section 12 presents reduced two-dimensional (2D) versions of the electromagnetic BIE system whose purpose is to facilitate some initial numerical tests and comparisons. Section 13 reviews test domains and discretization techniques and Section 14 presents numerical examples, including what we believe is the first high-order accurate computation of a surface plasmon wave on a non-smooth three-dimensional (3D) scatterer.

Appendix A presents boundary values of integral representations. Appendix B and C derive the conditions for the representations of the electric and magnetic fields to satisfy Maxwell's equations. In Appendix D a set of

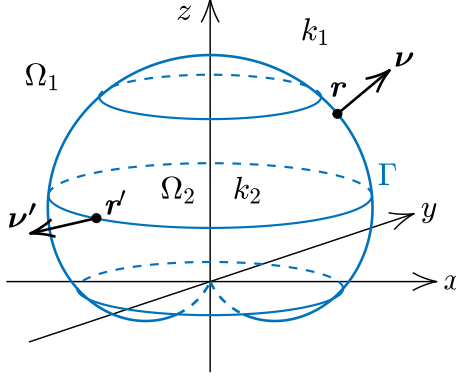


Figure 1: Geometry in \mathbb{R}^3 . Inside Γ the volume is Ω_2 and the wavenumber k_2 . Outside Γ the volume is Ω_1 and the wavenumber k_1 . The outward unit normal is ν at r and ν' at r' .

points $(\text{Arg}(k_1), \text{Arg}(k_2))$ is identified for which the PDE formulation of the electromagnetic transmission problem has at most one solution.

2 Notation

Let Ω_2 be a bounded volume in \mathbb{R}^3 with a smooth closed surface Γ and simply-connected unbounded exterior Ω_1 . The outward unit normal at position r on Γ is ν . We consider time-harmonic fields with time dependence e^{-it} , where the angular frequency is scaled to one. The relation between time-dependent fields $F(r, t)$ and complex fields $F(r)$ is

$$F(r, t) = \Re \{ F(r) e^{-it} \}. \quad (2)$$

The volumes Ω_1 and Ω_2 are homogeneous with constant material parameters and their wavenumbers are k_1 and k_2 . An incident field is generated by a source somewhere in Ω_1 . See Figure 1, where we depict a non-smooth Γ that will be used later in numerical examples.

2.1 Layer potentials and boundary integral operators

The fundamental solution to the scalar Helmholtz equation is taken to be

$$\Phi_k(r, r') = \frac{e^{ik|r-r'|}}{4\pi|r-r'|}, \quad r, r' \in \mathbb{R}^3. \quad (3)$$

Two scalar-valued layer potentials are defined in terms of a general surface density σ as

$$S_k \sigma(\mathbf{r}) = 2 \int_{\Gamma} \Phi_k(\mathbf{r}, \mathbf{r}') \sigma(\mathbf{r}') d\Gamma', \quad \mathbf{r} \in \Omega_1 \cup \Omega_2, \quad (4)$$

$$K_k \sigma(\mathbf{r}) = 2 \int_{\Gamma} (\partial_{\nu'} \Phi_k)(\mathbf{r}, \mathbf{r}') \sigma(\mathbf{r}') d\Gamma', \quad \mathbf{r} \in \Omega_1 \cup \Omega_2, \quad (5)$$

where $d\Gamma$ is an element of surface area, $\partial_{\nu'} = \boldsymbol{\nu}' \cdot \nabla'$, and $\boldsymbol{\nu}' = \boldsymbol{\nu}(\mathbf{r}')$. We shall use (4) and (5) also for $\mathbf{r} \in \Gamma$, in which case S_k and K_k are viewed as boundary integral operators. Further, we need the operators K_k^A and T_k , defined by

$$K_k^A \sigma(\mathbf{r}) = 2 \int_{\Gamma} (\partial_{\nu} \Phi_k)(\mathbf{r}, \mathbf{r}') \sigma(\mathbf{r}') d\Gamma', \quad \mathbf{r} \in \Gamma, \quad (6)$$

$$T_k \sigma(\mathbf{r}) = 2 \int_{\Gamma} (\partial_{\nu} \partial_{\nu'} \Phi_k)(\mathbf{r}, \mathbf{r}') \sigma(\mathbf{r}') d\Gamma', \quad \mathbf{r} \in \Gamma, \quad (7)$$

and where $T_k \sigma$ is to be understood in the Hadamard finite-part sense. We also need the vector-valued layer potentials

$$\mathcal{S}_k \boldsymbol{\sigma}(\mathbf{r}) = 2 \int_{\Gamma} \Phi_k(\mathbf{r}, \mathbf{r}') \boldsymbol{\sigma}(\mathbf{r}') d\Gamma', \quad \mathbf{r} \in \Omega_1 \cup \Omega_2, \quad (8)$$

$$\mathcal{N}_k \boldsymbol{\sigma}(\mathbf{r}) = 2 \int_{\Gamma} \nabla \Phi_k(\mathbf{r}, \mathbf{r}') \boldsymbol{\sigma}(\mathbf{r}') d\Gamma', \quad \mathbf{r} \in \Omega_1 \cup \Omega_2, \quad (9)$$

$$\mathcal{R}_k \boldsymbol{\sigma}(\mathbf{r}) = 2 \int_{\Gamma} \nabla \Phi_k(\mathbf{r}, \mathbf{r}') \times \boldsymbol{\sigma}(\mathbf{r}') d\Gamma', \quad \mathbf{r} \in \Omega_1 \cup \Omega_2, \quad (10)$$

with corresponding operators \mathcal{S}_k , \mathcal{N}_k , and \mathcal{R}_k for $\mathbf{r} \in \Gamma$. The notation

$$\begin{aligned} \tilde{S}_k &= ik_1 S_k, \\ \tilde{S}_k &= ik_1 S_k, \end{aligned} \quad (11)$$

will be used for brevity.

The fundamental solution Φ_k and the operators S_k , K_k , K_k^A , and T_k are identical to the corresponding constructs in [4, Eqs. (2.1) and (3.8)–(3.11)]. The layer potentials in (8), (9), and (10) correspond to the potentials in [24, Eqs. (3) and (9)], scaled with a factor of two.

2.2 Limits of layer potentials

It is convenient to introduce the notation

$$\begin{aligned} A^+(\mathbf{r}^\circ) &= \lim_{\Omega_1 \ni \mathbf{r} \rightarrow \mathbf{r}^\circ} A(\mathbf{r}), \quad \mathbf{r}^\circ \in \Gamma, \\ A^-(\mathbf{r}^\circ) &= \lim_{\Omega_2 \ni \mathbf{r} \rightarrow \mathbf{r}^\circ} A(\mathbf{r}), \quad \mathbf{r}^\circ \in \Gamma, \end{aligned} \quad (12)$$

for limits of a function $A(\mathbf{r})$ as $\Omega_1 \cup \Omega_2 \ni \mathbf{r} \rightarrow \mathbf{r}^\circ \in \Gamma$. For compositions of operators and functions, square brackets $[\cdot]$ indicate parts where limits are taken. In this notation, results from classical potential theory on limits of layer potentials include [4, Theorem 3.1] and [3, Theorem 2.23]

$$[S_k \sigma]^\pm(\mathbf{r}) = S_k \sigma(\mathbf{r}), \quad \mathbf{r} \in \Gamma, \quad (13)$$

$$[K_k \sigma]^\pm(\mathbf{r}) = \pm \sigma(\mathbf{r}) + K_k \sigma(\mathbf{r}), \quad \mathbf{r} \in \Gamma, \quad (14)$$

$$\boldsymbol{\nu} \cdot [\nabla S_k \sigma]^\pm(\mathbf{r}) = \mp \sigma(\mathbf{r}) + K_k^A \sigma(\mathbf{r}), \quad \mathbf{r} \in \Gamma, \quad (15)$$

$$\boldsymbol{\nu} \cdot [\nabla K_k \sigma]^\pm(\mathbf{r}) = T_k \sigma(\mathbf{r}), \quad \mathbf{r} \in \Gamma. \quad (16)$$

See also [14, Theorem 5.46] for statements on the limits (14) and (16) in a more modern function-space setting.

The layer potentials of (8), (9), and (10) have limits

$$[\mathcal{S}_k \boldsymbol{\sigma}]^\pm(\mathbf{r}) = \mathcal{S}_k \boldsymbol{\sigma}(\mathbf{r}), \quad \mathbf{r} \in \Gamma, \quad (17)$$

$$\boldsymbol{\nu} \cdot [\mathcal{N}_k \boldsymbol{\sigma}]^\pm(\mathbf{r}) = \mp \boldsymbol{\sigma}(\mathbf{r}) + \boldsymbol{\nu} \cdot \mathcal{N}_k \boldsymbol{\sigma}(\mathbf{r}), \quad \mathbf{r} \in \Gamma, \quad (18)$$

$$\boldsymbol{\nu} \times [\mathcal{R}_k \boldsymbol{\sigma}]^\pm(\mathbf{r}) = \pm \boldsymbol{\sigma}(\mathbf{r}) + \boldsymbol{\nu} \times \mathcal{R}_k \boldsymbol{\sigma}(\mathbf{r}), \quad \mathbf{r} \in \Gamma. \quad (19)$$

3 Scalar transmission problems

We present three scalar transmission problems called problem A, problem A₀, and problem B₀. Problem A is the problem of main interest. Problem A₀ and B₀ are needed in proofs.

3.1 Problem A and A₀

The transmission problem A reads: find $U(\mathbf{r})$, $\mathbf{r} \in \Omega_1 \cup \Omega_2$, which, for wavenumbers k_1 and k_2 such that

$$0 \leq \text{Arg}(k_1), \text{Arg}(k_2) < \pi, \quad (20)$$

solves

$$\Delta U(\mathbf{r}) + k_1^2 U(\mathbf{r}) = 0, \quad \mathbf{r} \in \Omega_1, \quad (21)$$

$$\Delta U(\mathbf{r}) + k_2^2 U(\mathbf{r}) = 0, \quad \mathbf{r} \in \Omega_2, \quad (22)$$

subject to the boundary conditions

$$U^+(\mathbf{r}) = U^-(\mathbf{r}), \quad \mathbf{r} \in \Gamma, \quad (23)$$

$$\kappa \boldsymbol{\nu} \cdot [\nabla U]^+(\mathbf{r}) = \boldsymbol{\nu} \cdot [\nabla U]^-(\mathbf{r}), \quad \mathbf{r} \in \Gamma, \quad (24)$$

$$(\partial_{|\mathbf{r}|} - ik_1) U^{\text{sc}}(\mathbf{r}) = o(|\mathbf{r}|^{-1}), \quad |\mathbf{r}| \rightarrow \infty. \quad (25)$$

Here κ is a parameter, the scattered field U^{sc} is given by

$$U(\mathbf{r}) = U^{\text{in}}(\mathbf{r}) + U^{\text{sc}}(\mathbf{r}), \quad \mathbf{r} \in \Omega_1, \quad (26)$$

and the incident field satisfies

$$\Delta U^{\text{in}}(\mathbf{r}) + k_1^2 U^{\text{in}}(\mathbf{r}) = 0, \quad \mathbf{r} \in \mathbb{R}^3, \quad (27)$$

except possibly at an isolated point in Ω_1 where the source of U^{in} is located.

The homogeneous version of problem A, that is problem A with $U^{\text{in}}=0$, is referred to as problem A_0 .

3.2 Problem B_0

The transmission problem B_0 reads: Find $W(\mathbf{r})$, $\mathbf{r} \in \Omega_1 \cup \Omega_2$, which, for wavenumbers k_1 and k_2 such that (20) holds, solves

$$\Delta W(\mathbf{r}) + k_2^2 W(\mathbf{r}) = 0, \quad \mathbf{r} \in \Omega_1, \quad (28)$$

$$\Delta W(\mathbf{r}) + k_1^2 W(\mathbf{r}) = 0, \quad \mathbf{r} \in \Omega_2, \quad (29)$$

subject to the boundary conditions

$$W^+(\mathbf{r}) = W^-(\mathbf{r}), \quad \mathbf{r} \in \Gamma, \quad (30)$$

$$\alpha \boldsymbol{\nu} \cdot [\nabla W]^+(\mathbf{r}) = \boldsymbol{\nu} \cdot [\nabla W]^-(\mathbf{r}), \quad \mathbf{r} \in \Gamma, \quad (31)$$

$$(\partial_{|\mathbf{r}|} - ik_2) W(\mathbf{r}) = o(|\mathbf{r}|^{-1}), \quad |\mathbf{r}| \rightarrow \infty, \quad (32)$$

where α is a parameter.

3.3 Uniqueness and existence

Uniqueness theorems for solutions to problem A are given by Kress and Roach [16] and by Kleinman and Martin [15]. We now review these theorems along with corollaries for problem A_0 and B_0 . Theorems and corollaries apply only under conditions on k_1 , k_2 , κ , and α that are more restrictive than those of (20). Conjugation of complex quantities is indicated with an overbar symbol.

3.3.1 Uniqueness theorem for problem A from [16, 15]

Theorem 3.1 in [16] says: Assume that (20) holds. Let in addition $k_1, k_2, \kappa, \kappa^{-1} \in \mathbb{C} \setminus 0$ be such that

$$\text{Arg}(k_1^2 \bar{k}_2^2 \kappa) = \begin{cases} 0 & \text{if } \Re\{k_1\} \Re\{k_2\} \geq 0, \\ \pi & \text{if } \Re\{k_1\} \Re\{k_2\} < 0. \end{cases} \quad (33)$$

Then problem A has at most one solution.

Remark 3.1. *There is a minor flaw in the proof of [16, Theorem 3.1]. As a consequence there are combinations of k_1 , k_2 and κ that satisfy (20) and (33), but for which problem A has nontrivial homogeneous solutions.*

Examples can be found by choosing $\text{Arg}(k_1) = \pi/2$, $\text{Arg}(k_2) = 0$, and $\text{Arg}(\kappa) = \pi$, and using the example for the sphere in [16, p. 1434]. To fix this problem one can supplement (33) with the condition

$$\text{Arg}(k_2) \neq 0 \quad \text{if} \quad \text{Arg}(k_1) = \pi/2. \quad (34)$$

The uniqueness theorem in [15, p. 309] says: Assume that (20) holds. Let in addition $k_1, k_2, \kappa, \kappa^{-1} \in \mathbb{C} \setminus 0$ be such that

$$0 \leq \text{Arg}(k_1 \kappa) \leq \pi \quad \text{and} \quad 0 \leq \text{Arg}(\bar{k}_1 k_2^2 \bar{\kappa}) \leq \pi. \quad (35)$$

Then problem A has at most one solution.

The conditions (35) intersect with the condition (33) and (34). If any of these sets of conditions holds, that is, if k_1, k_2 , and κ are such that (33) and (34) hold, or (35) holds, or all conditions hold, then we say that *the conditions of Section 3.3.1 hold*. These conditions are sufficient for our purposes but, as pointed out in [16, p. 1434], uniqueness can be established for a wider range of conditions.

Remark 3.2. In Ref. [15], the condition (20) is not directly included in the formulation of what corresponds to our problem A. Instead, the condition $0 \leq \text{Arg}(k_1) < \pi$ is added for the problem to have at most one solution and $0 \leq \text{Arg}(k_2) < \pi$ is added for the existence of a unique solution.

3.3.2 Uniqueness and existence of solutions to problem A_0

The conditions of Section 3.3.1 guarantee that problem A_0 has only the trivial solution $U(\mathbf{r}) = 0$.

3.3.3 Uniqueness and existence of solutions to problems A and A_0 when $\kappa = k_2^2/k_1^2$

The parameter value $\kappa = k_2^2/k_1^2$ is relevant for the electromagnetic transmission problem. By using similar techniques as in [15, 16] one can show that when $\kappa = k_2^2/k_1^2$ and $(\text{Arg}(k_1), \text{Arg}(k_2))$ is in the set of points of Figure 2(a), then problem A has at most one solution and problem A_0 has only the trivial solution $U(\mathbf{r}) = 0$.

We also mention that stronger results, including existence results, are available for problem A with (20) extended to $0 \leq \text{Arg}(k_1), \text{Arg}(k_2) \leq \pi$. Using methods from [1], developed for the more general theory of Dirac equations, one can prove that problem A has at most one solution in finite energy norm for $(\text{Arg}(k_1), \text{Arg}(k_2))$ in the set of points of Figure 2(b). Furthermore, such solutions exist in Lipschitz domains given that $k_2^2/k_1^2 \notin [-c_\Gamma, -1/c_\Gamma]$, where $c_\Gamma \geq 1$ is a geometry-dependent constant which assumes the value $c_\Gamma = 1$ for smooth Γ [Andreas Rosén, private communication 2019] and [1].

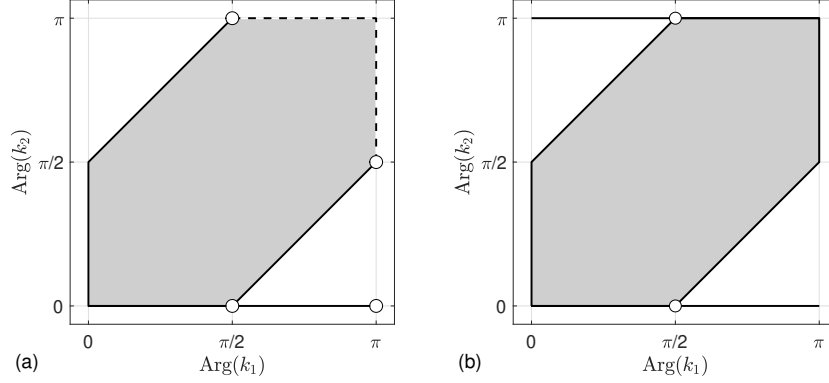


Figure 2: The gray regions and the solid black lines constitute the set of points $(\text{Arg}(k_1), \text{Arg}(k_2))$ for which, when $\kappa = k_2^2/k_1^2$, problem A has at most one solution and problem A_0 only has the trivial solution. Dashed lines and circles are not included. (a) A set of points obtained by extending the techniques used in [16]. (b) The set of points discussed in the second paragraph of Section 3.3.3.

3.3.4 Uniqueness and existence of solutions to problem B_0

If we interchange k_1 and k_2 , and replace κ by α in the conditions of Section 3.3.1, then we get sufficient conditions for which problem B_0 has only the trivial solution $W(\mathbf{r}) = 0$. The conditions (33) from Section 3.3.1 become

$$\text{Arg}(\bar{k}_1^2 k_2^2 \alpha) = \begin{cases} 0 & \text{if } \Re\{k_1\}\Re\{k_2\} \geq 0, \\ \pi & \text{if } \Re\{k_1\}\Re\{k_2\} < 0, \end{cases} \quad (36)$$

and

$$\text{Arg}(k_1) \neq 0 \quad \text{if} \quad \text{Arg}(k_2) = \pi/2. \quad (37)$$

The conditions (35) from Section 3.3.1 become

$$0 \leq \text{Arg}(k_2 \alpha) \leq \pi \quad \text{and} \quad 0 \leq \text{Arg}(k_1^2 \bar{k}_2 \bar{\alpha}) \leq \pi. \quad (38)$$

If any of these sets of conditions holds we say that *the conditions of Section 3.3.4 hold*.

4 Integral representations for problem A

We make an ansatz for two fields

$$U_1(\mathbf{r}) = \frac{1}{2}K_{k_1}\mu(\mathbf{r}) - \frac{1}{2}S_{k_1}\varrho(\mathbf{r}) + U^{\text{in}}(\mathbf{r}), \quad \mathbf{r} \in \Omega_1 \cup \Omega_2, \quad (39)$$

$$U_2(\mathbf{r}) = -\frac{1}{2}K_{k_2}\mu(\mathbf{r}) + \frac{\kappa}{2}S_{k_2}\varrho(\mathbf{r}), \quad \mathbf{r} \in \Omega_1 \cup \Omega_2, \quad (40)$$

where μ and ϱ are unknown layer densities. The relations in Section 2.2 give limits of U_1 and U_2 at $\mathbf{r} \in \Gamma$

$$U_1^+(\mathbf{r}) = \frac{1}{2}\mu(\mathbf{r}) + \frac{1}{2}K_{k_1}\mu(\mathbf{r}) - \frac{1}{2}S_{k_1}\varrho(\mathbf{r}) + U^{\text{in}}(\mathbf{r}), \quad (41)$$

$$U_1^-(\mathbf{r}) = U_1^+(\mathbf{r}) - \mu(\mathbf{r}), \quad (42)$$

$$U_2^+(\mathbf{r}) = -\frac{1}{2}\mu(\mathbf{r}) - \frac{1}{2}K_{k_2}\mu(\mathbf{r}) + \frac{\kappa}{2}S_{k_2}\varrho(\mathbf{r}), \quad (43)$$

$$U_2^-(\mathbf{r}) = U_2^+(\mathbf{r}) + \mu(\mathbf{r}). \quad (44)$$

Limits for the normal derivatives of U_1 and U_2 at $\mathbf{r} \in \Gamma$ are

$$\boldsymbol{\nu} \cdot [\nabla U_1]^+(\mathbf{r}) = \frac{1}{2}\varrho(\mathbf{r}) + \frac{1}{2}T_{k_1}\mu(\mathbf{r}) - \frac{1}{2}K_{k_1}^A\varrho(\mathbf{r}) + \boldsymbol{\nu} \cdot \nabla U^{\text{in}}(\mathbf{r}), \quad (45)$$

$$\boldsymbol{\nu} \cdot [\nabla U_1]^-(\mathbf{r}) = \boldsymbol{\nu} \cdot [\nabla U_1]^+(\mathbf{r}) - \varrho(\mathbf{r}), \quad (46)$$

$$\boldsymbol{\nu} \cdot [\nabla U_2]^+(\mathbf{r}) = -\frac{\kappa}{2}\varrho(\mathbf{r}) - \frac{1}{2}T_{k_2}\mu(\mathbf{r}) + \frac{\kappa}{2}K_{k_2}^A\varrho(\mathbf{r}), \quad (47)$$

$$\boldsymbol{\nu} \cdot [\nabla U_2]^-(\mathbf{r}) = \boldsymbol{\nu} \cdot [\nabla U_2]^+(\mathbf{r}) + \kappa\varrho(\mathbf{r}). \quad (48)$$

We now form the integral representation

$$U(\mathbf{r}) = \begin{cases} U_1(\mathbf{r}), & \mathbf{r} \in \Omega_1, \\ U_2(\mathbf{r}), & \mathbf{r} \in \Omega_2, \end{cases} \quad (49)$$

for the solution to problem A. The fundamental solution (3) makes U of (49) automatically satisfy the partial differential equations (21) and (22) and the radiation condition (25). It remains to determine μ and ϱ to ensure that the boundary conditions (23) and (24) are satisfied.

5 Integral equations for problem A

We propose the system of second kind integral equations

$$\begin{bmatrix} I - \beta_1(K_{k_1} - c_1K_{k_2}) & \beta_1(S_{k_1} - c_1\kappa S_{k_2}) \\ -\beta_2(T_{k_1} - c_2\kappa^{-1}T_{k_2}) & I + \beta_2(K_{k_1}^A - c_2K_{k_2}^A) \end{bmatrix} \begin{bmatrix} \mu(\mathbf{r}) \\ \varrho(\mathbf{r}) \end{bmatrix} = 2 \begin{bmatrix} \beta_1 U^{\text{in}}(\mathbf{r}) \\ \beta_2 \partial_{\boldsymbol{\nu}} U^{\text{in}}(\mathbf{r}) \end{bmatrix} \quad (50)$$

for the determination of μ and ϱ . Here I is the identity and

$$\beta_i = (1 + c_i)^{-1}, \quad i = 1, 2, \quad (51)$$

where c_i , $i = 1, 2$, are two free parameters such that

$$c_i \neq -1, 0. \quad (52)$$

We now prove that a solution $\{\mu, \varrho\}$ to (50), under certain conditions and via U of (49), represents a solution to problem A. Since U of (49)

satisfies (21), (22), and (25) for any $\{\mu, \varrho\}$, it remains to show that $\{\mu, \varrho\}$ from (50) makes U satisfy (23) and (24). For this we need to show that, under certain conditions, U_1 of (39) is zero in Ω_2 and U_2 of (40) is zero in Ω_1 . We introduce the auxiliary field

$$W(\mathbf{r}) = \begin{cases} U_2(\mathbf{r}), & \mathbf{r} \in \Omega_1, \\ -c_1^{-1}U_1(\mathbf{r}), & \mathbf{r} \in \Omega_2. \end{cases} \quad (53)$$

The field W of (53), with $\{\mu, \varrho\}$ from (50) and U_1 and U_2 from (39) and (40), is the unique solution to problem B_0 with $\alpha = c_2/(c_1\kappa)$ provided that the conditions of Section 3.3.4 hold. This is so since W , by construction, satisfies (28), (29), and (32). Furthermore, the boundary conditions (30) and (31) are satisfied. This can be checked by substituting (42), with (41), and (43) into (30), and (46), with (45), and (47) into (31), and using (50). As a consequence, according to Section 3.3.4, we have

$$W(\mathbf{r}) = 0, \quad \mathbf{r} \in \Omega_1 \cup \Omega_2. \quad (54)$$

From (53) and (54) it follows that $U_1 = 0$ in Ω_2 and that $U_2 = 0$ in Ω_1 . From this, several useful results follow for $\mathbf{r} \in \Gamma$. For example,

$$U_1^-(\mathbf{r}) = 0, \quad (55)$$

$$U_2^+(\mathbf{r}) = 0, \quad (56)$$

$$\boldsymbol{\nu} \cdot [\nabla U_1]^-(\mathbf{r}) = 0, \quad (57)$$

$$\boldsymbol{\nu} \cdot [\nabla U_2]^+(\mathbf{r}) = 0. \quad (58)$$

Now, from (42) and (55), and from (44) and (56)

$$U_1^+(\mathbf{r}) = \mu(\mathbf{r}), \quad (59)$$

$$U_2^-(\mathbf{r}) = \mu(\mathbf{r}). \quad (60)$$

Similarly, from (46) and (57), and from (48) and (58)

$$\boldsymbol{\nu} \cdot [\nabla U_1]^+(\mathbf{r}) = \varrho(\mathbf{r}), \quad (61)$$

$$\kappa^{-1}\boldsymbol{\nu} \cdot [\nabla U_2]^-(\mathbf{r}) = \varrho(\mathbf{r}). \quad (62)$$

It is now easy to see that (23) and (24) are satisfied and we conclude:

Theorem 5.1. *Assume that $\{k_1, k_2, \alpha = c_2/(c_1\kappa)\}$ are such that the conditions of Section 3.3.4 hold. Then a solution $\{\mu, \varrho\}$ to (50) represents, via (49), a solution also to problem A. Furthermore, (49) and (50) correspond to a direct integral equation formulation of problem A with μ and ϱ linked to limits of U and ∇U via (59), (60), (61), and (62).*

6 Unique solution to problem A from (50)

We use the Fredholm alternative to prove that, under certain conditions, the system (50) has a unique solution $\{\mu, \varrho\}$ and that this solution represents, via (49), the unique solution to problem A. Three conditions will be referred to with roman numerals

- (i) $c_2 = \kappa$ and (52) holds.
- (ii) k_1, k_2 , and κ make the conditions of Section 3.3.1 hold or, if $\kappa = k_2^2/k_1^2$, $(\text{Arg}(k_1), \text{Arg}(k_2))$ are in the set of points of Figure 2(a).
- (iii) k_1, k_2 , and $\alpha = c_2/(c_1\kappa)$ make the conditions of Section 3.3.4 hold.

We start with the observation that (50) is a Fredholm second kind integral equation with compact (differences of) operators when condition (i) holds. Then the Fredholm alternative can be applied to (50).

Let μ_0 and ϱ_0 be solutions to the homogeneous version of (50). Let U_{10} , U_0 , and W_0 be the fields (39), (49) and (53) with $\mu = \mu_0$ and $\varrho = \varrho_0$. From Section 5 we know that $W_0 = 0$ if (iii) holds. We shall now prove that also $U_0 = 0$ and, from that, $\mu_0 = 0$ and $\varrho_0 = 0$.

It follows from Theorem 5.1, which requires (iii), that $\{\mu_0, \varrho_0\}$ represents a solution to problem A₀. If (ii) holds, then $U_0 = 0$ according to Section 3.3.2. It then follows that $U_{10} = 0$ in Ω_1 so that $U_{10}^+ = 0$ and $[\nabla U_{10}]^+ = 0$. Then $\mu_0 = 0$ and $\varrho_0 = 0$ from (59) and (61).

Now, from the Fredholm alternative, the system (50) has a unique solution $\{\mu, \varrho\}$. By Theorem 5.1 this solution represents a solution to problem A. If problem A has at most one solution, which requires (ii), this solution to problem A is unique and we conclude:

Theorem 6.1. *Assume that conditions (i), (ii), and (iii) hold. Then the system (50) has a unique solution $\{\mu, \varrho\}$ which represents the unique solution to problem A.*

Note that, when (i) holds, $\alpha = 1/c_1$ in (iii) and it is always possible to find a constant c_1 so that (38) holds under the assumption (20). In this respect, condition (iii) in Theorem 6.1 does not introduce any additional constraint to problem A. A simple rule that satisfies condition (iii) is

$$c_1 = \begin{cases} e^{i\text{Arg}(k_2)} & \text{if } \Re\{k_1\} \geq 0, \\ e^{i(\text{Arg}(k_2)-\pi)} & \text{if } \Re\{k_1\} < 0. \end{cases} \quad (63)$$

This rule gives $c_1 = i$ when $(\text{Arg}(k_1), \text{Arg}(k_2)) = (0, \pi/2)$. It is also possible to choose $c_1 = -i$ when $(\text{Arg}(k_1), \text{Arg}(k_2)) = (0, \pi/2)$.

Our results, so far, extend those of [15, Section 4.1], where a direct formulation of problem A is presented in [15, Eq. (4.10)]. To see this, note that [15, Eq. (4.10)] corresponds to (50) with $c_2 = \kappa$ and $c_1 = 1/\kappa$. Now (50)

with $c_2 = \kappa$ and c_1 in agreement with (38) provides unique solutions over a broader range of k_1 , k_2 , and κ than does [15, Eq. (4.10)]. For example, if $(\text{Arg}(k_1), \text{Arg}(k_2)) = (0, \pi/2)$ and $\text{Arg}(\kappa) = \pi$, then (50) with $c_2 = \kappa$ and $c_1 = \pm i$ is guaranteed to have a unique solution while [15, Eq. (4.10)] is not.

7 Evaluation of the field U

Once the solution $\{\mu, \varrho\}$ has been obtained from (50), the field $U(\mathbf{r})$ can be evaluated via (49). When the field point \mathbf{r} is far away from Γ , the kernels of the layer potentials in (39) and (40) are smooth functions of \mathbf{r}' and any high-order discretization scheme should work well. When \mathbf{r} is close to Γ , the situation is more problematic due to the rapid variation with \mathbf{r}' in the Cauchy-type singular kernels of K_{k_1} and K_{k_2} . To alleviate this problem we introduce the field

$$V(\mathbf{r}) = \begin{cases} U_2(\mathbf{r}), & \mathbf{r} \in \Omega_1, \\ U_1(\mathbf{r}), & \mathbf{r} \in \Omega_2, \end{cases} \quad (64)$$

with U_1 and U_2 from (39) and (40). From (53) and (54) it follows that V is a null-field such that $V = 0$ in both Ω_1 and Ω_2 and hence $U = U + V$. The Cauchy-type kernel singularities in the representation of the combined field $U + V$ cancel out and we are left with weakly singular kernels which are easier to deal with numerically. Therefore, when \mathbf{r} is far away from Γ we evaluate U via (49). When \mathbf{r} is close to Γ we evaluate $U + V$ via (49) and (64).

8 Electromagnetic transmission problems

We present three electromagnetic transmission problems called problem C, problem C_0 , and problem D_0 . The main problem is C, whereas problems C_0 and D_0 are needed in proofs.

The prerequisites in Section 2 hold, with regions Ω_1 and Ω_2 that are dielectric and non-magnetic. The electric field is denoted \mathbf{E} and the magnetic field \mathbf{H} . The electric field is scaled such that $\mathbf{E} = \eta_1^{-1} \mathbf{E}_{\text{unscaled}}$, where $\eta_1 = \sqrt{\mu_0/\varepsilon_1}$ is the wave impedance of Ω_1 and ε_1 is the permittivity of Ω_1 . The parameter κ , introduced in (24), now has the value $\kappa = \varepsilon_2/\varepsilon_1$, where ε_2 is the permittivity of Ω_2 . For non-magnetic materials, this is equivalent to

$$\kappa = k_2^2/k_1^2. \quad (65)$$

8.1 Problems C and C_0

The transmission problem C reads: find $\mathbf{E}(\mathbf{r})$, $\mathbf{H}(\mathbf{r})$, $\mathbf{r} \in \Omega_1 \cup \Omega_2$, which, for wavenumbers k_1 and k_2 such that

$$0 \leq \text{Arg}(k_1), \text{Arg}(k_2) < \pi \quad \text{and} \quad \kappa \neq -1, \quad (66)$$

solve Maxwell's equations

$$\nabla \times \mathbf{E}(\mathbf{r}) = ik_1 \mathbf{H}(\mathbf{r}), \quad \mathbf{r} \in \Omega_1 \cup \Omega_2, \quad (67)$$

$$\nabla \times \mathbf{H}(\mathbf{r}) = -ik_1 \mathbf{E}(\mathbf{r}), \quad \mathbf{r} \in \Omega_1, \quad (68)$$

$$\nabla \times \mathbf{H}(\mathbf{r}) = -ik_1 \kappa \mathbf{E}(\mathbf{r}), \quad \mathbf{r} \in \Omega_2, \quad (69)$$

subject to the boundary conditions

$$\boldsymbol{\nu} \times \mathbf{E}^+(\mathbf{r}) = \boldsymbol{\nu} \times \mathbf{E}^-(\mathbf{r}), \quad \mathbf{r} \in \Gamma, \quad (70)$$

$$\boldsymbol{\nu} \times \mathbf{H}^+(\mathbf{r}) = \boldsymbol{\nu} \times \mathbf{H}^-(\mathbf{r}), \quad \mathbf{r} \in \Gamma, \quad (71)$$

$$(\partial_{|\mathbf{r}|} - ik_1) \mathbf{H}^{\text{sc}}(\mathbf{r}) = o(|\mathbf{r}|^{-1}), \quad |\mathbf{r}| \rightarrow \infty. \quad (72)$$

The scattered field is defined by

$$\mathbf{H}(\mathbf{r}) = \mathbf{H}^{\text{in}}(\mathbf{r}) + \mathbf{H}^{\text{sc}}(\mathbf{r}), \quad \mathbf{r} \in \Omega_1, \quad (73)$$

and the incident field satisfies

$$\nabla \times \mathbf{E}^{\text{in}}(\mathbf{r}) = ik_1 \mathbf{H}^{\text{in}}(\mathbf{r}), \quad \mathbf{r} \in \Omega_1 \cup \Omega_2, \quad (74)$$

$$\nabla \times \mathbf{H}^{\text{in}}(\mathbf{r}) = -ik_1 \mathbf{E}^{\text{in}}(\mathbf{r}), \quad \mathbf{r} \in \Omega_1 \cup \Omega_2, \quad (75)$$

except possibly at an isolated point in Ω_1 . The condition (72) and decomposition (73) also hold for \mathbf{E} .

The homogeneous problem \mathbf{C}_0 is problem \mathbf{C} with $\mathbf{E}^{\text{in}} = \mathbf{H}^{\text{in}} = \mathbf{0}$.

8.2 Problem \mathbf{D}_0

The transmission problem \mathbf{D}_0 reads: find $\mathbf{E}_W(\mathbf{r})$, $\mathbf{H}_W(\mathbf{r})$, $\mathbf{r} \in \Omega_1 \cup \Omega_2$, which, for wavenumbers k_1 and k_2 such that (66) holds, solve

$$\nabla \times \mathbf{E}_W(\mathbf{r}) = ik_1 \mathbf{H}_W(\mathbf{r}), \quad \mathbf{r} \in \Omega_1 \cup \Omega_2, \quad (76)$$

$$\nabla \times \mathbf{H}_W(\mathbf{r}) = -ik_1 \kappa \mathbf{E}_W(\mathbf{r}), \quad \mathbf{r} \in \Omega_1, \quad (77)$$

$$\nabla \times \mathbf{H}_W(\mathbf{r}) = -ik_1 \mathbf{E}_W(\mathbf{r}), \quad \mathbf{r} \in \Omega_2, \quad (78)$$

subject to the boundary conditions

$$\lambda \kappa \boldsymbol{\nu} \times \mathbf{E}_W^+(\mathbf{r}) = \boldsymbol{\nu} \times \mathbf{E}_W^-(\mathbf{r}), \quad \mathbf{r} \in \Gamma, \quad (79)$$

$$\boldsymbol{\nu} \times \mathbf{H}_W^+(\mathbf{r}) = \boldsymbol{\nu} \times \mathbf{H}_W^-(\mathbf{r}), \quad \mathbf{r} \in \Gamma, \quad (80)$$

$$(\partial_{|\mathbf{r}|} - ik_2) \mathbf{H}_W(\mathbf{r}) = o(|\mathbf{r}|^{-1}), \quad |\mathbf{r}| \rightarrow \infty. \quad (81)$$

Here λ is a parameter. The radiation condition (81) also holds for \mathbf{E}_W .

8.3 Uniqueness and existence of solutions to problem C, C_0 , and D_0

In Appendix D it is shown that when $(\text{Arg}(k_1), \text{Arg}(k_2))$ is in the set of points of Figure 2(a), then problem C has at most one solution and problem C_0 has only the trivial solution $\mathbf{E} = \mathbf{H} = \mathbf{0}$. It is also shown that when the conditions of Section 3.3.4 hold for $\{k_1, k_2, \alpha = \lambda\}$, then problem D_0 has only the trivial solution $\mathbf{E}_W = \mathbf{H}_W = \mathbf{0}$.

The stronger results for problem A, discussed in Section 3.3.3, carry over to problem C. One can prove that there exist unique solutions in finite energy norm to problem C in Lipschitz domains when $(\text{Arg}(k_1), \text{Arg}(k_2))$ is in the set of points of Figure 2(b) and k_2^2/k_1^2 is outside a certain interval on the real axis [Andreas Rosén, private communication (2019)] and [1].

9 Integral representations for problem C

Let σ_E , ϱ_E , \mathbf{M}_s , \mathbf{J}_s , ϱ_M , and σ_M be six unknown (scalar- and vector-valued) layer densities and define the four fields

$$\begin{aligned} \mathbf{E}_1(\mathbf{r}) = & -\frac{1}{2}\mathcal{N}_{k_1}\varrho_E(\mathbf{r}) - \frac{1}{2}\mathcal{R}_{k_1}(\nu'\sigma_M + \mathbf{M}_s)(\mathbf{r}) \\ & + \frac{1}{2}\tilde{\mathcal{S}}_{k_1}(\nu'\sigma_E + \mathbf{J}_s)(\mathbf{r}) + \mathbf{E}^{\text{in}}(\mathbf{r}), \quad \mathbf{r} \in \Omega_1 \cup \Omega_2, \end{aligned} \quad (82)$$

$$\begin{aligned} \mathbf{E}_2(\mathbf{r}) = & \frac{1}{2\kappa}\mathcal{N}_{k_2}\varrho_E(\mathbf{r}) + \frac{1}{2\kappa}\mathcal{R}_{k_2}(\nu'\sigma_M + \kappa\mathbf{M}_s)(\mathbf{r}) \\ & - \frac{1}{2}\tilde{\mathcal{S}}_{k_2}(\kappa^{-1}\nu'\sigma_E + \mathbf{J}_s)(\mathbf{r}), \quad \mathbf{r} \in \Omega_1 \cup \Omega_2, \end{aligned} \quad (83)$$

and

$$\begin{aligned} \mathbf{H}_1(\mathbf{r}) = & \frac{1}{2}\tilde{\mathcal{S}}_{k_1}(\nu'\sigma_M + \mathbf{M}_s)(\mathbf{r}) + \frac{1}{2}\mathcal{R}_{k_1}(\nu'\sigma_E + \mathbf{J}_s)(\mathbf{r}) \\ & - \frac{1}{2}\mathcal{N}_{k_1}\varrho_M(\mathbf{r}) + \mathbf{H}^{\text{in}}(\mathbf{r}), \quad \mathbf{r} \in \Omega_1 \cup \Omega_2, \end{aligned} \quad (84)$$

$$\begin{aligned} \mathbf{H}_2(\mathbf{r}) = & -\frac{1}{2}\tilde{\mathcal{S}}_{k_2}(\nu'\sigma_M + \kappa\mathbf{M}_s)(\mathbf{r}) - \frac{1}{2}\mathcal{R}_{k_2}(\kappa^{-1}\nu'\sigma_E + \mathbf{J}_s)(\mathbf{r}) \\ & + \frac{1}{2}\mathcal{N}_{k_2}\varrho_M(\mathbf{r}), \quad \mathbf{r} \in \Omega_1 \cup \Omega_2. \end{aligned} \quad (85)$$

Boundary limits of these representations are given in Appendix A. The notation $\tilde{\mathcal{S}}$ and $\tilde{\mathcal{S}}$ was introduced in (11). The introduction of the densities σ_E and σ_M is inspired by the integral representations for the generalized Helmholtz transmission problem in [27, 28].

The integral representations for problem C are

$$\mathbf{E}(\mathbf{r}) = \begin{cases} \mathbf{E}_1(\mathbf{r}), & \mathbf{r} \in \Omega_1, \\ \mathbf{E}_2(\mathbf{r}), & \mathbf{r} \in \Omega_2, \end{cases} \quad (86)$$

and

$$\mathbf{H}(\mathbf{r}) = \begin{cases} \mathbf{H}_1(\mathbf{r}), & \mathbf{r} \in \Omega_1, \\ \mathbf{H}_2(\mathbf{r}), & \mathbf{r} \in \Omega_2. \end{cases} \quad (87)$$

10 Integral equations for problem C

For the determination of $\{\sigma_E, \varrho_E, \mathbf{M}_s, \mathbf{J}_s, \varrho_M, \sigma_M\}$ we propose the system of second kind integral equations

$$\begin{bmatrix} I + \mathbf{Q}_{EE} & \mathbf{Q}_{EH} \\ \mathbf{Q}_{HE} & I + \mathbf{Q}_{HH} \end{bmatrix} \begin{bmatrix} \boldsymbol{\mu}_E \\ \boldsymbol{\mu}_H \end{bmatrix} = \begin{bmatrix} \mathbf{f}_E \\ \mathbf{f}_H \end{bmatrix}. \quad (88)$$

Here I is the identity and

$$\boldsymbol{\mu}_E = \begin{bmatrix} \sigma_E \\ \varrho_E \\ \mathbf{M}_s \end{bmatrix}, \quad \boldsymbol{\mu}_H = \begin{bmatrix} \mathbf{J}_s \\ \varrho_M \\ \sigma_M \end{bmatrix}, \quad (89)$$

$$\mathbf{f}_E = 2 \begin{bmatrix} 0 \\ \beta_4 \boldsymbol{\nu} \cdot \mathbf{E}^{\text{in}} \\ -\beta_5 \boldsymbol{\nu} \times \mathbf{E}^{\text{in}} \end{bmatrix}, \quad \mathbf{f}_H = 2 \begin{bmatrix} \beta_6 \boldsymbol{\nu} \times \mathbf{H}^{\text{in}} \\ \beta_7 \boldsymbol{\nu} \cdot \mathbf{H}^{\text{in}} \\ 0 \end{bmatrix}, \quad (90)$$

$$\begin{aligned} \mathbf{Q}_{EE} &= \begin{bmatrix} -\beta_3(K_{k_1} - c_3 K_{k_2}) & -\beta_3(\tilde{S}_{k_1} - c_3 \kappa \tilde{S}_{k_2}) & 0 \\ -\beta_4 \boldsymbol{\nu} \cdot (\tilde{S}_{k_1} - c_4 \tilde{S}_{k_2}) \boldsymbol{\nu}' & \beta_4(K_{k_1}^A - c_4 K_{k_2}^A) & \beta_4 \boldsymbol{\nu} \cdot (\mathcal{R}_{k_1} - c_4 \kappa \mathcal{R}_{k_2}) \\ \beta_5 \boldsymbol{\nu} \times (\tilde{S}_{k_1} - c_5 \kappa^{-1} \tilde{S}_{k_2}) \boldsymbol{\nu}' & -\beta_5 \boldsymbol{\nu} \times (\mathcal{N}_{k_1} - c_5 \kappa^{-1} \mathcal{N}_{k_2}) & -\beta_5 \boldsymbol{\nu} \times (\mathcal{R}_{k_1} - c_5 \kappa \mathcal{R}_{k_2}) \end{bmatrix}, \\ \mathbf{Q}_{EH} &= \begin{bmatrix} \beta_3 \nabla \cdot (\mathcal{S}_{k_1} - c_3 \kappa \mathcal{S}_{k_2}) & 0 & 0 \\ -\beta_4 \boldsymbol{\nu} \cdot (\tilde{S}_{k_1} - c_4 \kappa \tilde{S}_{k_2}) & 0 & \beta_4 \boldsymbol{\nu} \cdot (\mathcal{R}_{k_1} - c_4 \kappa \mathcal{R}_{k_2}) \boldsymbol{\nu}' \\ \beta_5 \boldsymbol{\nu} \times (\tilde{S}_{k_1} - c_5 \tilde{S}_{k_2}) & 0 & -\beta_5 \boldsymbol{\nu} \times (\mathcal{R}_{k_1} - c_5 \kappa^{-1} \mathcal{R}_{k_2}) \boldsymbol{\nu}' \end{bmatrix}, \\ \mathbf{Q}_{HE} &= \begin{bmatrix} -\beta_6 \boldsymbol{\nu} \times (\mathcal{R}_{k_1} - c_6 \kappa^{-1} \mathcal{R}_{k_2}) \boldsymbol{\nu}' & 0 & -\beta_6 \boldsymbol{\nu} \times (\tilde{S}_{k_1} - c_6 \kappa \tilde{S}_{k_2}) \\ -\beta_7 \boldsymbol{\nu} \cdot (\mathcal{R}_{k_1} - c_7 \kappa^{-1} \mathcal{R}_{k_2}) \boldsymbol{\nu}' & 0 & -\beta_7 \boldsymbol{\nu} \cdot (\tilde{S}_{k_1} - c_7 \kappa \tilde{S}_{k_2}) \\ 0 & 0 & \beta_8 \nabla \cdot (\mathcal{S}_{k_1} - c_8 \kappa \mathcal{S}_{k_2}) \end{bmatrix}, \\ \mathbf{Q}_{HH} &= \begin{bmatrix} -\beta_6 \boldsymbol{\nu} \times (\mathcal{R}_{k_1} - c_6 \mathcal{R}_{k_2}) & \beta_6 \boldsymbol{\nu} \times (\mathcal{N}_{k_1} - c_6 \mathcal{N}_{k_2}) & -\beta_6 \boldsymbol{\nu} \times (\tilde{S}_{k_1} - c_6 \tilde{S}_{k_2}) \boldsymbol{\nu}' \\ -\beta_7 \boldsymbol{\nu} \cdot (\mathcal{R}_{k_1} - c_7 \mathcal{R}_{k_2}) & \beta_7 (K_{k_1}^A - c_7 K_{k_2}^A) & -\beta_7 \boldsymbol{\nu} \cdot (\tilde{S}_{k_1} - c_7 \tilde{S}_{k_2}) \boldsymbol{\nu}' \\ 0 & -\beta_8 (\tilde{S}_{k_1} - c_8 \kappa \tilde{S}_{k_2}) & -\beta_8 (K_{k_1} - c_8 K_{k_2}) \end{bmatrix}, \end{aligned} \quad (91)$$

where

$$\begin{aligned} \beta_i &= (1 + c_i)^{-1}, \quad i = 3, \dots, 8, \\ c_3 &= \gamma_E c, \quad c_4 = c_6 = c, \quad c_5 = c_7 = \lambda \kappa c, \quad c_8 = \gamma_M c, \end{aligned} \quad (92)$$

and c, λ, γ_E , and γ_M are free parameters such that

$$c_i \neq -1, 0, \quad i = 3, \dots, 8. \quad (93)$$

10.1 Criteria for (86) and (87) to represent a solution to problem C

We now prove that a solution $\{\boldsymbol{\mu}_E, \boldsymbol{\mu}_H\}$ to (88), under certain conditions and via (86) and (87), represents a solution to problem C.

The fundamental solution (3) makes \mathbf{E} and \mathbf{H} of (86) and (87) satisfy the radiation condition (72). It remains to prove that \mathbf{E} and \mathbf{H} satisfy Maxwell's equations (67), (68), and (69) and the boundary conditions (70) and (71). For this we first need to show that, under certain conditions, \mathbf{E}_1 and \mathbf{H}_1 of (82) and (84) are zero in Ω_2 and \mathbf{E}_2 and \mathbf{H}_2 of (83) and (85) are zero in Ω_1 . We introduce the auxiliary fields

$$\mathbf{E}_W(\mathbf{r}) = \begin{cases} \mathbf{E}_2(\mathbf{r}), & \mathbf{r} \in \Omega_1, \\ -c^{-1}\mathbf{E}_1(\mathbf{r}), & \mathbf{r} \in \Omega_2, \end{cases} \quad (94)$$

and

$$\mathbf{H}_W(\mathbf{r}) = \begin{cases} \mathbf{H}_2(\mathbf{r}), & \mathbf{r} \in \Omega_1, \\ -c^{-1}\mathbf{H}_1(\mathbf{r}), & \mathbf{r} \in \Omega_2. \end{cases} \quad (95)$$

The fields \mathbf{E}_W and \mathbf{H}_W of (94) and (95), with $\{\sigma_E, \varrho_E, \mathbf{M}_s, \mathbf{J}_s, \varrho_M, \sigma_M\}$ from (88), is the unique trivial solution to problem D_0 provided the sets $\{k_1, k_2, \alpha = \lambda\bar{\gamma}_M\}$, $\{k_1, k_2, \alpha = \bar{\gamma}_E\bar{\kappa}\}$, and $\{k_1, k_2, \alpha = \lambda\}$ are such that the conditions of Section 3.3.4 hold. This is now shown in several steps. The fundamental solution (3) makes \mathbf{E}_W and \mathbf{H}_W satisfy (81). Using Appendix A in combination with (88) one can show that (79) and (80) are satisfied. Appendix B shows that if $\{\boldsymbol{\mu}_E, \boldsymbol{\mu}_H\}$ is a solution to (88) and if the conditions of Section 3.3.4 hold for $\{k_1, k_2, \alpha = \lambda\bar{\gamma}_M\}$ and $\{k_1, k_2, \alpha = \bar{\gamma}_E\bar{\kappa}\}$, then

$$\nabla \cdot \mathbf{E}_W(\mathbf{r}) = 0, \quad \mathbf{r} \in \Omega_1 \cup \Omega_2, \quad (96)$$

$$\nabla \cdot \mathbf{H}_W(\mathbf{r}) = 0, \quad \mathbf{r} \in \Omega_1 \cup \Omega_2. \quad (97)$$

Appendix C shows that if (96) and (97) hold, then \mathbf{E}_W and \mathbf{H}_W satisfy (76), (77), and (78). By that we have shown that (94) and (95) satisfy problem D_0 when $\{\boldsymbol{\mu}_E, \boldsymbol{\mu}_H\}$ is a solution to (88) and $\{k_1, k_2, \alpha = \lambda\bar{\gamma}_M\}$ and $\{k_1, k_2, \alpha = \bar{\gamma}_E\bar{\kappa}\}$ are such that the conditions of Section 3.3.4 hold. If the conditions of Section 3.3.4 also hold for $\{k_1, k_2, \alpha = \lambda\}$, then D_0 only has the trivial solution $\mathbf{E}_W = \mathbf{H}_W = \mathbf{0}$, that is

$$\begin{aligned} \mathbf{E}_2(\mathbf{r}) = \mathbf{H}_2(\mathbf{r}) &= \mathbf{0}, & \mathbf{r} \in \Omega_1, \\ \mathbf{E}_1(\mathbf{r}) = \mathbf{H}_1(\mathbf{r}) &= \mathbf{0}, & \mathbf{r} \in \Omega_2. \end{aligned} \quad (98)$$

From (98) and Appendix A we obtain boundary values of the integral

representations (86) and (87)

$$[\nabla \cdot \mathbf{E}_1]^+(\mathbf{r}) = \kappa[\nabla \cdot \mathbf{E}_2]^-(\mathbf{r}) = -ik_1\sigma_E(\mathbf{r}), \quad (99)$$

$$\boldsymbol{\nu} \cdot \mathbf{E}_1^+(\mathbf{r}) = \kappa\boldsymbol{\nu} \cdot \mathbf{E}_2^-(\mathbf{r}) = \varrho_E(\mathbf{r}), \quad (100)$$

$$\boldsymbol{\nu} \times \mathbf{E}_1^+(\mathbf{r}) = \boldsymbol{\nu} \times \mathbf{E}_2^-(\mathbf{r}) = -\mathbf{M}_s(\mathbf{r}), \quad (101)$$

$$\boldsymbol{\nu} \times \mathbf{H}_1^+(\mathbf{r}) = \boldsymbol{\nu} \times \mathbf{H}_2^-(\mathbf{r}) = \mathbf{J}_s(\mathbf{r}), \quad (102)$$

$$\boldsymbol{\nu} \cdot \mathbf{H}_1^+(\mathbf{r}) = \boldsymbol{\nu} \cdot \mathbf{H}_2^-(\mathbf{r}) = \varrho_M(\mathbf{r}), \quad (103)$$

$$[\nabla \cdot \mathbf{H}_1]^+(\mathbf{r}) = [\nabla \cdot \mathbf{H}_2]^-(\mathbf{r}) = -ik_1\sigma_M(\mathbf{r}). \quad (104)$$

Due to (101) and (102), \mathbf{E} and \mathbf{H} of (86) and (87) satisfy (70) and (71). Appendix B shows that (99)–(104) imply

$$\begin{aligned} \nabla \cdot \mathbf{E}(\mathbf{r}) &= 0, & \mathbf{r} &\in \Omega_1 \cup \Omega_2, \\ \nabla \cdot \mathbf{H}(\mathbf{r}) &= 0, & \mathbf{r} &\in \Omega_1 \cup \Omega_2. \end{aligned} \quad (105)$$

Finally, from the representations (82)–(85) and the divergence condition (105), Appendix C shows that (67), (68), and (69) are satisfied. We conclude:

Theorem 10.1. *Assume that $\{k_1, k_2, \alpha = \lambda\bar{\gamma}_M\}$, $\{k_1, k_2, \alpha = \bar{\gamma}_E\bar{\kappa}\}$, and $\{k_1, k_2, \alpha = \lambda\}$ are such that the conditions of Section 3.3.4 hold. Then a solution $\{\boldsymbol{\mu}_E, \boldsymbol{\mu}_H\}$ to (88) represents, via (86) and (87), a solution also to problem C. Furthermore, (86), (87), and (88) correspond to a direct integral equation formulation of problem C with $\{\boldsymbol{\mu}_E, \boldsymbol{\mu}_H\}$ linked to limits of \mathbf{E} and \mathbf{H} via (99)–(104).*

Remark 10.1. *The layer densities in (99)–(104) can be given the following physical interpretations: $-ik_1\sigma_E$ and $-ik_1\sigma_M$ are the electric and magnetic volume charge densities at Γ^+ , ϱ_E and ϱ_M are the equivalent electric and magnetic surface charge densities on Γ^+ , and \mathbf{M}_s and \mathbf{J}_s are the equivalent magnetic and electric surface current densities on Γ^+ .*

11 Unique solution to problem C from (88)

We now prove that if there exists a solution to problem C, then, under certain conditions, there exists a solution $\{\boldsymbol{\mu}_E, \boldsymbol{\mu}_H\}$ to (88) and it represents the unique solution to problem C. Three conditions will be referred to with roman numerals

- (i) The conditions in (93) hold.
- (ii) $(\text{Arg}(k_1), \text{Arg}(k_2))$ are in the set of points of Figure 2(a).
- (iii) $\{k_1, k_2, \alpha = \lambda\bar{\gamma}_M\}$, $\{k_1, k_2, \alpha = \bar{\gamma}_E\bar{\kappa}\}$, and $\{k_1, k_2, \alpha = \lambda\}$ are such that the conditions of Section 3.3.4 hold.

Let $\{\boldsymbol{\mu}_{E0}, \boldsymbol{\mu}_{H0}\}$ be the solution to the homogeneous version of (88) and assume that (i), (ii), and (iii) hold. According to Section 8.3 problem C_0 only has the trivial solution $\boldsymbol{E} = \boldsymbol{H} = \mathbf{0}$, since (ii) holds. The limits of fields in (99)–(104) are then zero and hence $\{\boldsymbol{\mu}_{E0}, \boldsymbol{\mu}_{H0}\}$ are zero. Then (88) has at most one solution $\{\boldsymbol{\mu}_E, \boldsymbol{\mu}_H\}$. Since $\{\boldsymbol{\mu}_E, \boldsymbol{\mu}_H\}$ is linked to limits of \boldsymbol{E} and \boldsymbol{H} via (99)–(104) it follows that if problem C has a solution, then via (99)–(104) this solution gives $\{\boldsymbol{\mu}_E, \boldsymbol{\mu}_H\}$ that solves (88). We conclude:

Theorem 11.1. *Assume that there exists a solution to problem C for k_1 and k_2 with arguments in the set of points of Figure 2(a). Then this solution is unique. If conditions (i), (ii), and (iii) hold then there exists a unique solution $\{\boldsymbol{\mu}_E, \boldsymbol{\mu}_H\}$ to (88), and this solution represents via (86) and (87) the unique solution to problem C.*

For positive frequencies all known materials are located in the square $0 \leq \text{Arg}(k_1), \text{Arg}(k_2) \leq \pi/2$. Except for the point $(\text{Arg}(k_1), \text{Arg}(k_2)) = (\pi/2, 0)$, the solution to problem C is unique in this physically important square.

Remark 11.1. *From (99), (104), and (105) it is seen that σ_E and σ_M are zero. Despite this, σ_E and σ_M are needed in (88) to guarantee uniqueness. Often, however, one can omit σ_E and σ_M from (88) and still get the correct unique solution.*

11.1 Determination of uniqueness parameters

The system (88) contains the free parameters λ , γ_E , γ_M , and c . Unique solvability of (88) requires that the conditions of Section 3.3.4 hold for the sets $\{k_1, k_2, \alpha = \lambda \bar{\gamma}_M\}$, $\{k_1, k_2, \alpha = \bar{\gamma}_E \bar{\kappa}\}$, and $\{k_1, k_2, \alpha = \lambda\}$ while the choice of c is restricted by (93). Because of their role in ensuring unique solvability of (88), we refer to $\{\lambda, \gamma_E, \gamma_M, c\}$ as *uniqueness parameters*.

Generally, there are many parameter choices for which the conditions of Section 3.3.4 and (93) hold for a given $\{k_1, k_2\}$ satisfying (20). A valid choice when $\text{Arg}(k_1) = 0$ and $0 \leq \text{Arg}(k_2) \leq \pi/2$ is

$$\lambda = e^{-i\text{Arg}(k_2)}, \quad \gamma_E = \kappa^{-1} e^{i(\text{Arg}(k_2) - \pi)}, \quad \gamma_M = 1, \quad c = \lambda^{-1}. \quad (106)$$

A valid choice when $\text{Arg}(k_1) = 0$ and $\pi/2 \leq \text{Arg}(k_2) < \pi$ is

$$\lambda = e^{i(\pi - \text{Arg}(k_2))}, \quad \gamma_E = \kappa^{-1} e^{i\text{Arg}(k_2)}, \quad \gamma_M = 1, \quad c = \lambda^{-1}. \quad (107)$$

12 2D limits

As a first numerical test of our formulations of the scalar and electromagnetic transmission problems we shall consider, in Section 14, the 2D transverse magnetic (TM) transmission problem where an incident transverse magnetic

wave is scattered from an infinitely long cylinder. This problem is independent of the z -coordinate and we introduce the vector $r = (x, y)$, the unit tangent vector $\tau = (\tau_x, \tau_y)$, and the unit normal vector $\nu = (\nu_x, \nu_y)$, where $(\tau_x, \tau_y, 0) = \hat{z} \times (\nu_x, \nu_y, 0)$ and \hat{z} is the unit vector in the z -direction. The incident wave has polarization $\mathbf{H}^{\text{in}}(r) = \hat{z}H^{\text{in}}(r)$, which implies $\mathbf{M}_s = \hat{z}M$, $\mathbf{J}_s = \tau J$, $\varrho_M = 0$, and $\sigma_M = 0$.

The integral representations (39), (40), and (82)–(85), as well as the systems (50) and (88), are transferred to two dimensions by exchanging the fundamental solution (3) for the 2D fundamental solution

$$\Phi_k(r, r') = \frac{i}{4}H_0^{(1)}(k|r - r'|), \quad r, r' \in \mathbb{R}^2, \quad (108)$$

where $H_0^{(1)}$ is the zeroth order Hankel function of the first kind.

12.1 Integral representations in two dimensions

Since σ_E is zero, the 2D representation of the field in (87), to be used in evaluation of the magnetic field, is

$$H(r) = \begin{cases} \frac{1}{2}\tilde{S}_{k_1}M(r) - \frac{1}{2}K_{k_1}J(r) + H^{\text{in}}(r), & r \in \Omega_1, \\ -\frac{\kappa}{2}\tilde{S}_{k_2}M(r) + \frac{1}{2}K_{k_2}J(r), & r \in \Omega_2. \end{cases} \quad (109)$$

By letting $U = H$, $U^{\text{in}} = H^{\text{in}}$, $\mu = -J$, $\varrho = -ik_1M$, and $\kappa = k_2^2/k_1^2$ in the scalar representation (49) it becomes identical to (109). According to Section 7 one may add the null-fields

$$0 = \begin{cases} -\frac{\kappa}{2}\tilde{S}_{k_2}M(r) + \frac{1}{2}K_{k_2}J(r), & r \in \Omega_1, \\ \frac{1}{2}\tilde{S}_{k_1}M(r) - \frac{1}{2}K_{k_1}J(r) + H^{\text{in}}(r), & r \in \Omega_2, \end{cases} \quad (110)$$

to (109). That gives the representation

$$H(r) = \frac{1}{2}(\tilde{S}_{k_1} - \kappa\tilde{S}_{k_2})M(r) - \frac{1}{2}(K_{k_1} - K_{k_2})J(r) + H^{\text{in}}(r), \quad r \in \Omega_1 \cup \Omega_2, \quad (111)$$

which is to prefer when evaluating the magnetic field at points r close to Γ .

12.2 Integral equations with four densities

In the TM problem the system (88) becomes

$$\begin{bmatrix} I + \mathbf{Q}_{EE} & \mathbf{Q}_{EH} \\ \mathbf{Q}_{HE} & I + \mathbf{Q}_{HH} \end{bmatrix} \begin{bmatrix} \mu_E \\ \mu_H \end{bmatrix} = \begin{bmatrix} f_E \\ f_H \end{bmatrix}, \quad (112)$$

where

$$\boldsymbol{\mu}_E = \begin{bmatrix} \sigma_E \\ \varrho_E \\ M \end{bmatrix}, \quad \mu_H = J, \quad (113)$$

$$\mathbf{f}_E = 2 \begin{bmatrix} 0 \\ \beta_4 i k_1^{-1} \partial_\tau H^{\text{in}} \\ \beta_5 i k_1^{-1} \partial_\nu H^{\text{in}} \end{bmatrix}, \quad f_H = -2\beta_6 H^{\text{in}}, \quad (114)$$

and

$$\begin{aligned} \mathbf{Q}_{EE} &= \begin{bmatrix} -\beta_3(K_{k_1} - c_3 K_{k_2}) & -\beta_3(\tilde{S}_{k_1} - c_3 \kappa \tilde{S}_{k_2}) & 0 \\ -\beta_4(\tilde{S}_{k_1} - c_4 \tilde{S}_{k_2}) \nu \cdot \nu' & \beta_4(K_{k_1}^A - c_4 K_{k_2}^A) & \beta_4(C_{k_1}^A - c_4 \kappa C_{k_2}^A) \\ \beta_5(\tilde{S}_{k_1} - c_5 \kappa^{-1} \tilde{S}_{k_2}) \tau \cdot \nu' & -\beta_5(C_{k_1}^A - c_5 \kappa^{-1} C_{k_2}^A) & \beta_5(K_{k_1}^A - c_5 K_{k_2}^A) \end{bmatrix}, \\ \mathbf{Q}_{EH} &= \begin{bmatrix} -\beta_3(C_{k_1} - c_3 \kappa C_{k_2}) \\ -\beta_4(\tilde{S}_{k_1} - c_4 \kappa \tilde{S}_{k_2}) \nu \cdot \tau' \\ \beta_5(\tilde{S}_{k_1} - c_5 \tilde{S}_{k_2}) \tau \cdot \tau' \end{bmatrix}, \\ \mathbf{Q}_{HE} &= [\beta_6(C_{k_1} - c_6 \kappa^{-1} C_{k_2}) \quad 0 \quad \beta_6(\tilde{S}_{k_1} - c_6 \kappa \tilde{S}_{k_2})], \\ Q_{HH} &= -\beta_6(K_{k_1} - c_6 K_{k_2}). \end{aligned} \quad (115)$$

Here

$$C_k \sigma(r) = 2 \int_\Gamma (\partial_{\tau'} \Phi_k)(r, r') \sigma(r') d\Gamma', \quad r \in \Gamma, \quad (116)$$

$$C_k^A \sigma(r) = 2 \int_\Gamma (\partial_\tau \Phi_k)(r, r') \sigma(r') d\Gamma', \quad r \in \Gamma. \quad (117)$$

12.3 Integral equations with three densities

If we omit σ_E , see Remark 11.1, the system (115) reduces to

$$\begin{aligned} & \begin{bmatrix} I + \beta_4(K_{k_1}^A - c_4 K_{k_2}^A) & \beta_4(C_{k_1}^A - c_4 \kappa C_{k_2}^A) & -\beta_4(\tilde{S}_{k_1} - c_4 \kappa \tilde{S}_{k_2}) \nu \cdot \tau' \\ -\beta_5(C_{k_1}^A - c_5 \kappa^{-1} C_{k_2}^A) & I + \beta_5(K_{k_1}^A - c_5 K_{k_2}^A) & \beta_5(\tilde{S}_{k_1} - c_5 \tilde{S}_{k_2}) \tau \cdot \tau' \\ 0 & \beta_6(\tilde{S}_{k_1} - c_6 \kappa \tilde{S}_{k_2}) & I - \beta_6(K_{k_1} - c_6 K_{k_2}) \end{bmatrix} \begin{bmatrix} \varrho_E \\ M \\ J \end{bmatrix} \\ &= 2 \begin{bmatrix} \beta_4 i k_1^{-1} \partial_\tau H^{\text{in}} \\ \beta_5 i k_1^{-1} \partial_\nu H^{\text{in}} \\ -\beta_6 H^{\text{in}} \end{bmatrix}. \end{aligned} \quad (118)$$

12.4 Integral equations with two densities

A third alternative is to only use the densities M and J . The integral representation (49) and system (50) are now suitable, where the change of

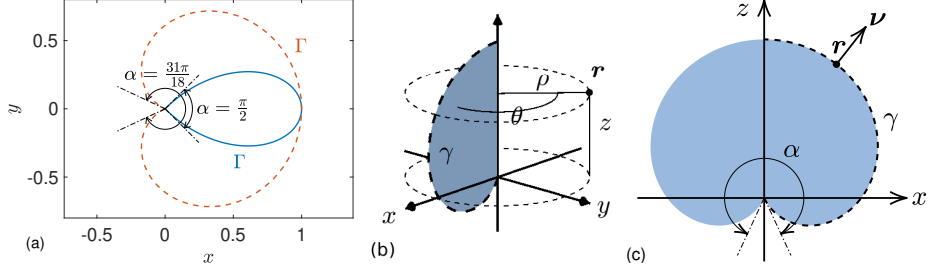


Figure 3: Non-smooth test domains: (a) boundaries Γ of 2D domains with corner opening angles $\alpha = \pi/2$ (solid blue) and $\alpha = 31\pi/18$ (dashed orange); (b) Cylindrical coordinates (ρ, θ, z) for a point \mathbf{r} on the surface of an axisymmetric object. The generating curve is γ ; (c) A cross section of the object generated by γ . The opening angle of the conical point at the origin is $\alpha = 31\pi/18$.

variables in Section 12.1 makes (49) equal to (109) and (50) equal to

$$\begin{bmatrix} I + \beta_2(K_{k_1}^A - c_2 K_{k_2}^A) & \beta_2 i k_1^{-1}(T_{k_1} - c_2 \kappa^{-1} T_{k_2}) \\ \beta_1(\tilde{S}_{k_1} - c_1 \kappa \tilde{S}_{k_2}) & I - \beta_1(K_{k_1} - c_1 K_{k_2}) \end{bmatrix} \begin{bmatrix} M \\ J \end{bmatrix} = 2 \begin{bmatrix} \beta_2 i k_1^{-1} \partial_\nu H^{\text{in}} \\ -\beta_1 H^{\text{in}} \end{bmatrix}. \quad (119)$$

If the conditions in Theorem 6.1 hold, then (119) has a unique solution $\{M, J\}$. Via (109) it represents the unique solution to the 2D TM problem.

13 Test domains and discretization

This section reviews domains and discretization schemes that are used for numerical tests in the next section.

13.1 The 2D one-corner object and the 3D “tomato”

Numerical tests in two dimensions involve a one-corner object whose boundary Γ is parameterized as

$$\mathbf{r}(s) = \sin(\pi s) (\cos((s - 0.5)\alpha), \sin((s - 0.5)\alpha)) , \quad s \in [0, 1], \quad (120)$$

and where α is a corner opening angle. See Figure 3(a) for illustrations.

Numerical tests in three dimensions involve an object whose surface Γ is created by revolving the generating curve γ , parameterized as

$$\mathbf{r}(s) = \sin(\pi s) (\sin((0.5 - s)\alpha), 0, \cos((0.5 - s)\alpha)) , \quad s \in [0, 0.5], \quad (121)$$

around the z -axis. For $\alpha > \pi$ this object resembles a “tomato”. See Figure 1 and Figure 3(b,c) for illustrations with $\alpha = 31\pi/18$.

The reason for testing integral equations in axisymmetric domains, rather than in general domains, relates to the availability of efficient high-order

solvers. Use of axisymmetric domains and solvers as a robust test-bed for new integral equation reformulations of scattering problems is contemporary common practice [6, 18]. Note that the choice $\alpha = \pi$ makes Γ from (120) become a circle and Γ from (121) a sphere.

13.2 RCIP-accelerated Nyström discretization schemes

Nyström discretization, relying on composite Gauss–Legendre quadrature, is used for all our systems of integral equations. Large discretized linear systems are solved iteratively using GMRES. In the presence of singular boundary points which call for intense mesh refinement, the Nyström scheme is accelerated by recursively compressed inverse preconditioning (RCIP) [8]. The RCIP acts as a fully automated, geometry-independent, and fast direct local solver and boosts the performance of the original Nyström scheme to the point where problems on non-smooth Γ are solved with the same ease and to the same precision as problems on smooth Γ . Accurate evaluations of layer potentials close to their sources on Γ are accomplished using variants of the techniques first presented in [7].

The schemes used in the numerical examples are not entirely new. For 2D problems we use the scheme in [11, Section 11.3], relying on 16-point composite quadrature. For 3D problems we use a modified unification of the schemes in [9] and [12], relying on 32-point composite quadrature. A key feature in the schemes of [9] and [12] is an FFT-accelerated separation of variables, pioneered by [29] and used also in [6, 18].

An important technique in the scheme of [9] is the split of the numerator in $\Phi_k(\mathbf{r}, \mathbf{r}')$ of (3) into parts that are even and odd in $|\mathbf{r} - \mathbf{r}'|$. Let $G(k, \mathbf{r}, \mathbf{r}')$ be one of the 2π -periodic kernels of Section 2.1. Azimuthal Fourier coefficients

$$G_n = \frac{1}{\sqrt{2\pi}} \int_{-\pi}^{\pi} e^{-in(\theta - \theta')} G(k, \mathbf{r}, \mathbf{r}') d(\theta - \theta'), \quad n = 0, \pm 1, \pm 2, \dots, \quad (122)$$

are, for \mathbf{r} and \mathbf{r}' close to each other, computed in different ways depending on the parity of these parts. When $\Im m\{k\}$ is small, the split

$$e^{ik|\mathbf{r} - \mathbf{r}'|} = \cos(k|\mathbf{r} - \mathbf{r}'|) + i \sin(k|\mathbf{r} - \mathbf{r}'|) \quad (123)$$

is efficient for $\Phi_k(\mathbf{r}, \mathbf{r}')$. When $\Im m\{k\}$ is large, the terms on the right hand side of (123) can be much larger in modulus than the function on the left hand side. Then numerical cancellation takes place. To fix this problem for large $\Im m\{k\}$, not encountered in [9], we introduce a bump-like function

$$\chi(k, |\mathbf{r} - \mathbf{r}'|) = e^{-(\Im m\{k\}|\mathbf{r} - \mathbf{r}'|/4.6)^8}, \quad (124)$$

modify the split (123) to

$$e^{ik|\mathbf{r} - \mathbf{r}'|} = (1 - \chi)e^{ik|\mathbf{r} - \mathbf{r}'|} + \chi \cos(k|\mathbf{r} - \mathbf{r}'|) + i\chi \sin(k|\mathbf{r} - \mathbf{r}'|), \quad (125)$$

and compute G_n of (122) with techniques (direct transform or convolution) appropriate for parts of $G(k, \mathbf{r}, \mathbf{r}')$ associated with each of the terms on the right hand side of (125).

14 Numerical examples

The systems (88), (112), (118), and (119) and the representations (86), (87), (109), and (111) are now put to the test. In all examples we take k_1 real and positive, $\varepsilon_1 = 1$, and $\varepsilon_2 = -1.1838$. This parameter combination has been used in previous work on surface plasmon waves [2, 10, 11]. It satisfies the plasmonic condition (1) and offers, by that, tough numerical challenges. In situations involving non-smooth surfaces, it may happen that solutions for $\varepsilon_2 = -1.1838$ do not exist. We then compute limit solutions as ε_2 approaches -1.1838 from above in the complex plane. Such limit solutions, discussed in the context of Laplace transmission problems in [12, Section 2.2], are given a downarrow superscript. For example, the limit of the field \mathbf{H} is denoted \mathbf{H}^\downarrow . The uniqueness parameters $\{\lambda, \gamma_E, \gamma_M, c\}$, needed in (88), (112), and (118), are chosen according to (107). The uniqueness parameters $\{c_1, c_2\}$, needed in (119), are chosen as $c_1 = -i$ and $c_2 = \kappa$.

Our codes are implemented in MATLAB, release 2018b, and executed on a workstation equipped with an Intel Core i7-3930K CPU and 64 GB of RAM. The implementations are standard and rely on built-in functions. When assessing the accuracy of computed field quantities we most often adopt a procedure where to each numerical solution we also compute an overresolved reference solution, using roughly 50% more points in the discretization of the system under study. The absolute difference between these two solutions is denoted the *estimated absolute error*. Throughout the examples, field quantities are computed at 10^6 field points on a rectangular Cartesian grid in the computational domains shown in the figures.

14.1 Unique solvability on the unit circle

We compute condition numbers of the discretized system matrices in (112), (118), and (119). The boundary Γ is the unit circle and k_1 is swept through the interval $[0, 10]$. Recall that the four-density system (112) and the two-density system (119) are guaranteed to be free from wavenumbers for which the solution is not unique (false eigenwavenumbers) while the three-density system (118) is not.

Condition number analysis of 2D-limits of 3D-systems on the unit circle is a revealing test for detecting if a given system of integral equations has false eigenwavenumbers when the plasmonic condition holds. For example, in [11, Figure 9] it is shown that the original Müller system and the “ \mathbf{E} -system” of [28] exhibit several false eigenwavenumbers in such a test, for which they are not guaranteed to work.

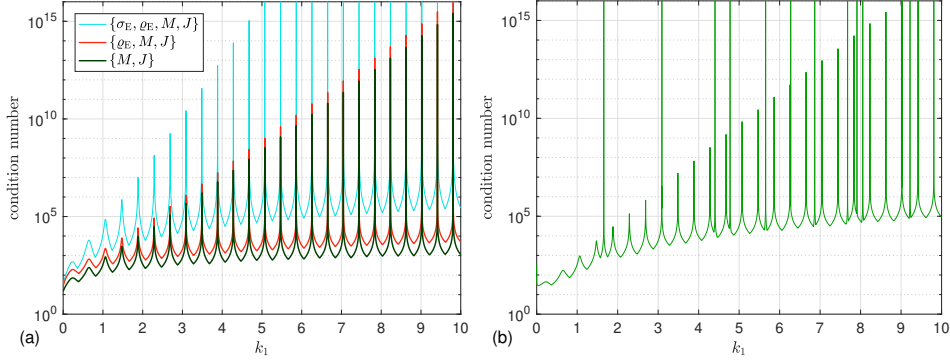


Figure 4: Condition numbers of system matrices on the unit circle, $\varepsilon_1 = 1$, $\varepsilon_2 = -1.1838$, and $k_1 \in [0, 10]$: (a) the systems (112), (118), and (119); (b) the Müller system.

Figure 4(a) shows results obtained with (112), (118), and (119) using 768 discretization points on Γ and approximately 20,700 values of $k_1 \in [0, 10]$ to resolve the three curves. The regularly recurring high peaks correspond to true eigenwavenumbers k_1 just below the positive k_1 -axis (weakly damped dynamic surface plasmons). One can see that neither the four-density system (112) nor the two-density system (119) exhibits any false eigenwavenumbers, as expected, and that (119) is the best conditioned system. Furthermore, which is more remarkable, the three-density system (118) also appears to be free from false eigenwavenumbers. For comparison, Figure 4(b) shows a result from [11, Figure 9], produced by the 2D-limit of the original Müller system. Here one can see twelve false eigenwavenumbers.

14.2 Field accuracy for the 2D one-corner object

An incident plane wave with $\mathbf{H}^{\text{in}}(r) = \hat{\mathbf{z}}e^{ik_1 d \cdot r}$, exterior wavenumber $k_1 = 18$, and direction of propagation $d = (\cos(\pi/4), \sin(\pi/4))$ is scattered against the 2D one-corner object of Section 13.1. The corner opening angle is $\alpha = \pi/2$. A number of 800 discretization points is placed on Γ and the performance of the three systems (112), (118), (119) along with the representation formulas (109) and (111) are compared.

Figure 5(a) shows the total magnetic field $H^\perp(r, t)$ at $t = 0$, compare (2), and Figures 5(b,c,d) show \log_{10} of the estimated absolute error obtained with (112), (118), and (119), respectively. The number of GMRES iterations required to solve the discretized linear systems is 266 for (112), 154 for (118), and 143 for (119). The absolute errors for the systems (112) and (118) are estimated using the solution from (119) as reference solution.

Several interesting observations can be made from Figure 5. Not only is the field accuracy high for all three systems. The number of digits lost is in agreement with what could be expected for computations on the unit circle,

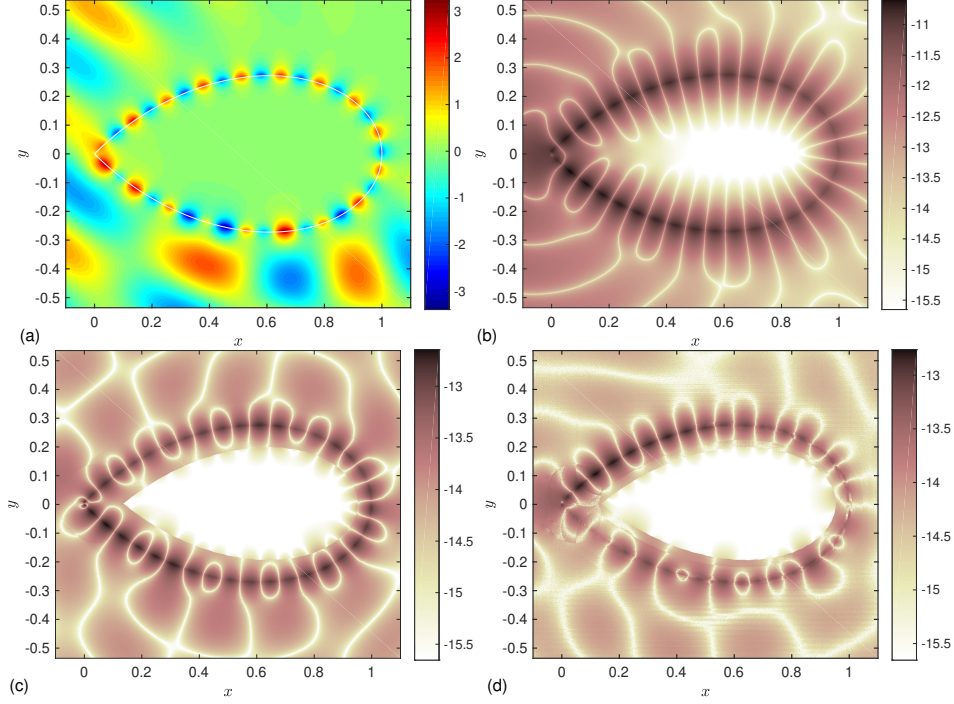


Figure 5: The field $H^\downarrow(r, 0)$ on the 2D one-corner object with $\varepsilon_1 = 1$, $\varepsilon_2 = -1.1838$, and $k_1 = 18$: (a) the field $H^\downarrow(r, 0)$ itself; (b,c,d) \log_{10} of estimated absolute field error using the systems (112), (118), and (119), respectively.

considering the condition numbers shown in Figure 4 and assuming that k_1 is not close to a true eigenwavenumber. This illustrates the ability of RCIP acceleration to erase most difficulties associated with Nyström discretization on non-smooth boundaries, as mentioned in Section 13.2.

Note also that (119) is a system of Fredholm second kind integral equations with compact (differences of) operators – a property often sought for in integral equation modeling of PDE:s. The system (118), on the other hand, contains a singular difference of integral operators. Still, the performance of the two systems is very similar.

14.3 Unique solvability on the unit sphere

We repeat the experiment of Section 14.1, but now on the unit sphere using the system (88). Inspired by the good performance of the system (118), reported above and where σ_E is omitted, we omit both σ_E and σ_M from (88) to get a six-scalar-density system. Again, there is no proof that this system has a unique solution, but every solution to the time harmonic Maxwell's equations corresponds to a solution to this system.

Figure 6(a) shows result for the azimuthal modes $n = 0, 5, 10$, with 768

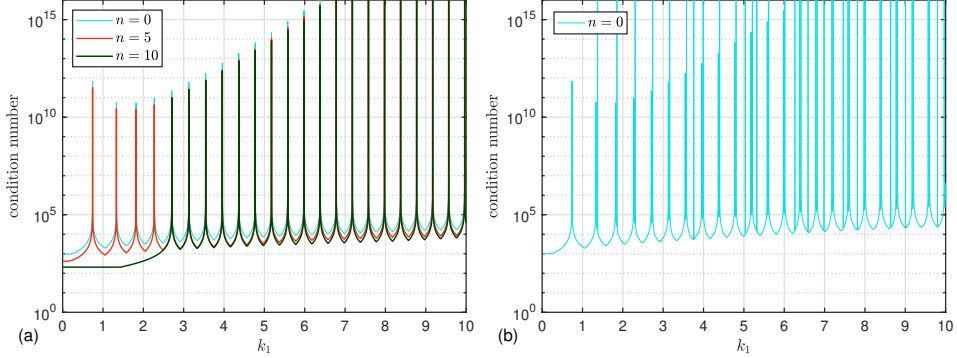


Figure 6: Condition numbers of system matrices on the unit sphere, $\varepsilon_1 = 1$, $\varepsilon_2 = -1.1838$, and $k_1 \in [0, 10]$: (a) the system (88) with σ_E and σ_M omitted; (b) the pseudo-Müller system.

discretization points on the generating curve γ , and with approximately 3,500 values of $k_1 \in [0, 10]$. No false eigenwavenumbers can be seen. For comparison, Figure 6(b) shows results for a six-scalar-density variant of the Müller system. The original four-scalar-density Müller system[22, p. 319] uses the surface current densities \mathbf{M}_s and \mathbf{J}_s and contains compact differences of hypersingular operators. These operator differences are quite hard to implement numerically in three dimensions, even though it definitely is possible on axisymmetric surfaces [18]. Our variant of the Müller system is derived from the original Müller system via integration by parts and relating the surface divergence of \mathbf{M}_s and \mathbf{J}_s to ϱ_M and ϱ_E , see [9, Eqs. (36) and (35)]. This corresponds to omitting both σ_E and σ_M from (88) and setting $c_4 = c_6 = 1$, and $c_5 = c_7 = \kappa$. Figure 6(b) shows that this pseudo-Müller system exhibits at least 32 false eigenwavenumbers for $k_1 \in [0, 10]$.

14.4 Field accuracy for the 3D “tomato”

An incident linearly polarized plane wave with $\mathbf{E}^{\text{in}}(\mathbf{r}) = \hat{\mathbf{x}}e^{ik_1 z}$ and $k_1 = 5$ is scattered against the 3D “tomato” of Section 13.1. The conical point opening angle is $\alpha = 31\pi/18$. The same six-scalar-density version of the system (88) is used as in Section 14.3. Only two azimuthal Fourier modes, $n = -1$ and $n = 1$, are present in this problem and the Fourier coefficients of the layer densities of these modes are either identical or have opposite signs. Therefore only one modal system needs to be solved numerically.

Figure 7 shows the electric field in the ρ -direction, $E_\rho^\perp(r, 0)$, and the magnetic field in the θ -direction, $H_\theta^\perp(r, 0)$, on the cross section in Figure 3(c). The results are obtained with 576 discretization points on the generating curve γ and with 242 GMRES iterations. The field $E_\rho^\perp(r, 0)$ is singular at the origin. Therefore the colorbar range in Figure 7(a) is restricted to the

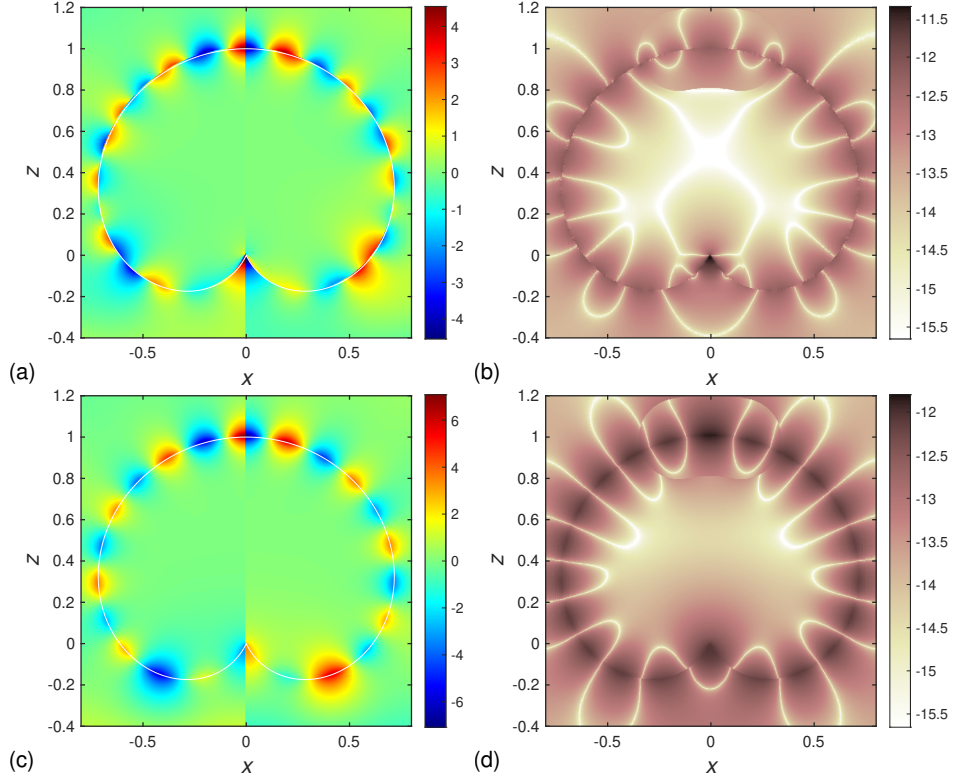


Figure 7: Field images on a cross section of the 3D “tomato” subjected to an incident plane wave $\mathbf{E}^{\text{in}}(\mathbf{r}) = \hat{\mathbf{x}}e^{ik_1z}$ and with $\varepsilon_1 = 1$, $\varepsilon_2 = -1.1838$, and $k_1 = 5$: (a) the field $E_\rho^\downarrow(r, 0)$ with colorbar range set to $[-4.55, 4.55]$; (b) \log_{10} of estimated absolute field error in $E_\rho^\downarrow(r, 0)$; (c) the field $H_\theta^\downarrow(r, 0)$; (d) \log_{10} of estimated absolute field error in $H_\theta^\downarrow(r, 0)$.

most extreme values of $E_\rho^\downarrow(r, 0)$ away from the origin. The precision shown in Figure 7(b,d) is consistent with the condition numbers of Figure 6(a) in the sense discussed in Section 14.2. We conclude by noting that Figure 7 clearly shows an accurately computed surface plasmon wave on a non-smooth 3D object in a setup with negative permittivity ratio. To simulate such surface waves is the ultimate goal of this work.

15 Conclusions

A new system of Fredholm second kind integral equations is presented for an electromagnetic transmission problem involving a single scattering object. Our work can be seen as an extension of the work by Kleinman and Martin [15] on direct methods for scalar transmission problems. Thanks to the introduction of certain uniqueness parameters, our new system gives unique

solutions for a wider range of wavenumber combinations k_1 and k_2 than do other systems of integral equations for Maxwell's equations, for example the original Müller system. In particular, unique solutions are guaranteed for smooth scatterers when the plasmonic condition (1) holds.

The favorable properties of our new system extend beyond what can be proven rigorously. In a numerical example, a reduced version of the system in combination with a high-order Fourier-Nyström discretization scheme is shown to produce accurate field images of a surface plasmon wave on a non-smooth axisymmetric scatterer.

Acknowledgement

We would like to thank Andreas Rosén (formerly Andreas Axelsson) for many useful conversations. This work was supported by the Swedish Research Council under contract 621-2014-5159.

Appendix

A. Boundary limits of $\mathbf{E}(\mathbf{r})$ and $\mathbf{H}(\mathbf{r})$

The relations in Section 2.2 give the following limits at $\mathbf{r} \in \Gamma$ for the integral representations of $\mathbf{E}(\mathbf{r})$ and $\mathbf{H}(\mathbf{r})$ in (82)–(85):

$$[\nabla \cdot \mathbf{E}_1]^+(\mathbf{r}) = -\frac{ik_1}{2}\sigma_E(\mathbf{r}) - \frac{ik_1}{2}\tilde{\mathcal{S}}_{k_1}\varrho_E(\mathbf{r}) + \frac{1}{2}\nabla \cdot \tilde{\mathcal{S}}_{k_1}(\boldsymbol{\nu}'\sigma_E + \mathbf{J}_s)(\mathbf{r}), \quad (\text{A.1})$$

$$[\nabla \cdot \mathbf{E}_1]^-(\mathbf{r}) = [\nabla \cdot \mathbf{E}_1]^+(\mathbf{r}) + ik_1\sigma_E(\mathbf{r}), \quad (\text{A.2})$$

$$\begin{aligned} \boldsymbol{\nu} \cdot \mathbf{E}_1^+(\mathbf{r}) &= \frac{1}{2}\varrho_E(\mathbf{r}) - \frac{1}{2}\boldsymbol{\nu} \cdot \mathcal{N}_{k_1}\varrho_E(\mathbf{r}) - \frac{1}{2}\boldsymbol{\nu} \cdot \mathcal{R}_{k_1}(\boldsymbol{\nu}'\sigma_M + \mathbf{M}_s)(\mathbf{r}) \\ &\quad + \frac{1}{2}\boldsymbol{\nu} \cdot \tilde{\mathcal{S}}_{k_1}(\boldsymbol{\nu}'\sigma_E + \mathbf{J}_s)(\mathbf{r}) + \boldsymbol{\nu} \cdot \mathbf{E}^{\text{in}}(\mathbf{r}), \end{aligned} \quad (\text{A.3})$$

$$\boldsymbol{\nu} \cdot \mathbf{E}_1^-(\mathbf{r}) = \boldsymbol{\nu} \cdot \mathbf{E}_1^+(\mathbf{r}) - \varrho_E(\mathbf{r}), \quad (\text{A.4})$$

$$\begin{aligned} \boldsymbol{\nu} \times \mathbf{E}_1^+(\mathbf{r}) &= -\frac{1}{2}\mathbf{M}_s(\mathbf{r}) - \frac{1}{2}\boldsymbol{\nu} \times \mathcal{N}_{k_1}\varrho_E(\mathbf{r}) - \frac{1}{2}\boldsymbol{\nu} \times \mathcal{R}_{k_1}(\boldsymbol{\nu}'\sigma_M + \mathbf{M}_s)(\mathbf{r}) \\ &\quad + \frac{1}{2}\boldsymbol{\nu} \times \tilde{\mathcal{S}}_{k_1}(\boldsymbol{\nu}'\sigma_E + \mathbf{J}_s)(\mathbf{r}) + \boldsymbol{\nu} \times \mathbf{E}^{\text{in}}(\mathbf{r}), \end{aligned} \quad (\text{A.5})$$

$$\boldsymbol{\nu} \times \mathbf{E}_1^-(\mathbf{r}) = \boldsymbol{\nu} \times \mathbf{E}_1^+(\mathbf{r}) + \mathbf{M}_s(\mathbf{r}), \quad (\text{A.6})$$

$$\begin{aligned} \boldsymbol{\nu} \times \mathbf{H}_1^+(\mathbf{r}) &= \frac{1}{2}\mathbf{J}_s(\mathbf{r}) + \frac{1}{2}\boldsymbol{\nu} \times \tilde{\mathcal{S}}_{k_1}(\boldsymbol{\nu}'\sigma_M + \mathbf{M}_s)(\mathbf{r}) \\ &\quad + \frac{1}{2}\boldsymbol{\nu} \times \mathcal{R}_{k_1}(\boldsymbol{\nu}'\sigma_E + \mathbf{J}_s)(\mathbf{r}) - \frac{1}{2}\boldsymbol{\nu} \times \mathcal{N}_{k_1}\varrho_M(\mathbf{r}) + \boldsymbol{\nu} \times \mathbf{H}^{\text{in}}(\mathbf{r}), \end{aligned} \quad (\text{A.7})$$

$$\boldsymbol{\nu} \times \mathbf{H}_1^-(\mathbf{r}) = \boldsymbol{\nu} \times \mathbf{H}_1^+(\mathbf{r}) - \mathbf{J}_s(\mathbf{r}), \quad (\text{A.8})$$

$$\boldsymbol{\nu} \cdot \mathbf{H}_1^+(\mathbf{r}) = \frac{1}{2}\varrho_M(\mathbf{r}) + \frac{1}{2}\boldsymbol{\nu} \cdot \tilde{\mathcal{S}}_{k_1}(\boldsymbol{\nu}'\sigma_M + \mathbf{M}_s)(\mathbf{r})$$

$$+\frac{1}{2}\boldsymbol{\nu}\cdot\mathcal{R}_{k_1}(\boldsymbol{\nu}'\sigma_E+\mathbf{J}_s)(\mathbf{r})-\frac{1}{2}\boldsymbol{\nu}\cdot\mathcal{N}_{k_1}\varrho_M(\mathbf{r})+\boldsymbol{\nu}\cdot\mathbf{H}^{\text{in}}(\mathbf{r}), \quad (\text{A.9})$$

$$\boldsymbol{\nu}\cdot\mathbf{H}_1^-(\mathbf{r})=\boldsymbol{\nu}\cdot\mathbf{H}_1^+(\mathbf{r})-\varrho_M(\mathbf{r}), \quad (\text{A.10})$$

$$[\nabla\cdot\mathbf{H}_1]^+(\mathbf{r})=-\frac{ik_1}{2}\sigma_M(\mathbf{r})+\frac{1}{2}\nabla\cdot\tilde{\mathcal{S}}_{k_1}(\boldsymbol{\nu}'\sigma_M+\mathbf{M}_s)(\mathbf{r})-\frac{ik_1}{2}\tilde{\mathcal{S}}_{k_1}\varrho_M(\mathbf{r}), \quad (\text{A.11})$$

$$[\nabla\cdot\mathbf{H}_1]^-(\mathbf{r})=[\nabla\cdot\mathbf{H}_1]^+(\mathbf{r})+ik_1\sigma_M(\mathbf{r}), \quad (\text{A.12})$$

and

$$[\nabla\cdot\mathbf{E}_2]^+(\mathbf{r})=\frac{ik_1}{2\kappa}\sigma_E(\mathbf{r})+\frac{ik_1}{2}\tilde{\mathcal{S}}_{k_2}\varrho_E(\mathbf{r})-\frac{1}{2}\nabla\cdot\tilde{\mathcal{S}}_{k_2}(\kappa^{-1}\boldsymbol{\nu}'\sigma_E+\mathbf{J}_s)(\mathbf{r}), \quad (\text{A.13})$$

$$[\nabla\cdot\mathbf{E}_2]^-(\mathbf{r})=[\nabla\cdot\mathbf{E}_2]^+(\mathbf{r})-ik_1\kappa^{-1}\sigma_E(\mathbf{r}), \quad (\text{A.14})$$

$$\begin{aligned} \boldsymbol{\nu}\cdot\mathbf{E}_2^+(\mathbf{r}) &= -\frac{1}{2\kappa}\varrho_E(\mathbf{r})+\frac{1}{2\kappa}\boldsymbol{\nu}\cdot\mathcal{N}_{k_2}\varrho_E(\mathbf{r})+\frac{1}{2\kappa}\boldsymbol{\nu}\cdot\mathcal{R}_{k_2}(\boldsymbol{\nu}'\sigma_M+\kappa\mathbf{M}_s)(\mathbf{r}) \\ &\quad -\frac{1}{2}\boldsymbol{\nu}\cdot\tilde{\mathcal{S}}_{k_2}(\kappa^{-1}\boldsymbol{\nu}'\sigma_E+\mathbf{J}_s)(\mathbf{r}), \end{aligned} \quad (\text{A.15})$$

$$\boldsymbol{\nu}\cdot\mathbf{E}_2^-(\mathbf{r})=\boldsymbol{\nu}\cdot\mathbf{E}_2^+(\mathbf{r})+\kappa^{-1}\varrho_E(\mathbf{r}), \quad (\text{A.16})$$

$$\begin{aligned} \boldsymbol{\nu}\times\mathbf{E}_2^+(\mathbf{r}) &= \frac{1}{2}\mathbf{M}_s(\mathbf{r})+\frac{1}{2\kappa}\boldsymbol{\nu}\times\mathcal{N}_{k_2}\varrho_E(\mathbf{r})+\frac{1}{2\kappa}\boldsymbol{\nu}\times\mathcal{R}_{k_2}(\boldsymbol{\nu}'\sigma_M+\kappa\mathbf{M}_s)(\mathbf{r}) \\ &\quad -\frac{1}{2}\boldsymbol{\nu}\times\tilde{\mathcal{S}}_{k_2}(\kappa^{-1}\boldsymbol{\nu}'\sigma_E+\mathbf{J}_s)(\mathbf{r}), \end{aligned} \quad (\text{A.17})$$

$$\boldsymbol{\nu}\times\mathbf{E}_2^-(\mathbf{r})=\boldsymbol{\nu}\times\mathbf{E}_2^+(\mathbf{r})-\mathbf{M}_s(\mathbf{r}), \quad (\text{A.18})$$

$$\begin{aligned} \boldsymbol{\nu}\times\mathbf{H}_2^+(\mathbf{r}) &= -\frac{1}{2}\mathbf{J}_s(\mathbf{r})-\frac{1}{2}\boldsymbol{\nu}\times\tilde{\mathcal{S}}_{k_2}(\boldsymbol{\nu}'\sigma_M+\kappa\mathbf{M}_s)(\mathbf{r}) \\ &\quad -\frac{1}{2}\boldsymbol{\nu}\times\mathcal{R}_{k_2}(\kappa^{-1}\boldsymbol{\nu}'\sigma_E+\mathbf{J}_s)(\mathbf{r})+\frac{1}{2}\boldsymbol{\nu}\times\mathcal{N}_{k_2}\varrho_M(\mathbf{r}), \end{aligned} \quad (\text{A.19})$$

$$\boldsymbol{\nu}\times\mathbf{H}_2^-(\mathbf{r})=\boldsymbol{\nu}\times\mathbf{H}_2^+(\mathbf{r})+\mathbf{J}_s(\mathbf{r}), \quad (\text{A.20})$$

$$\begin{aligned} \boldsymbol{\nu}\cdot\mathbf{H}_2^+(\mathbf{r}) &= -\frac{1}{2}\varrho_M(\mathbf{r})-\frac{1}{2}\boldsymbol{\nu}\cdot\tilde{\mathcal{S}}_{k_2}(\boldsymbol{\nu}'\sigma_M+\kappa\mathbf{M}_s)(\mathbf{r}) \\ &\quad -\frac{1}{2}\boldsymbol{\nu}\cdot\mathcal{R}_{k_2}(\kappa^{-1}\boldsymbol{\nu}'\sigma_E+\mathbf{J}_s)(\mathbf{r})+\frac{1}{2}\boldsymbol{\nu}\cdot\mathcal{N}_{k_2}\varrho_M(\mathbf{r}), \end{aligned} \quad (\text{A.21})$$

$$\boldsymbol{\nu}\cdot\mathbf{H}_2^-(\mathbf{r})=\boldsymbol{\nu}\cdot\mathbf{H}_2^+(\mathbf{r})+\varrho_M(\mathbf{r}), \quad (\text{A.22})$$

$$[\nabla\cdot\mathbf{H}_2]^+(\mathbf{r})=\frac{ik_1}{2}\sigma_M(\mathbf{r})-\frac{1}{2}\nabla\cdot\tilde{\mathcal{S}}_{k_2}(\boldsymbol{\nu}'\sigma_M+\kappa\mathbf{M}_s)(\mathbf{r})+\frac{ik_1}{2}\kappa\tilde{\mathcal{S}}_{k_2}\varrho_M(\mathbf{r}), \quad (\text{A.23})$$

$$[\nabla\cdot\mathbf{H}_2]^-(\mathbf{r})=[\nabla\cdot\mathbf{H}_2]^+(\mathbf{r})-ik_1\sigma_M(\mathbf{r}). \quad (\text{A.24})$$

B. Divergence conditions

We first derive necessary conditions for (97) to hold, when \mathbf{E}_W and \mathbf{H}_W are defined through (94) and (95), (82)–(85), and the solution to (88). The conditions for (96) and (105) to hold follow by using the same technique.

The limits in Appendix A and (88) give the boundary relations

$$\lambda\kappa\boldsymbol{\nu} \times \mathbf{E}_W^+(\mathbf{r}) = \boldsymbol{\nu} \times \mathbf{E}_W^-(\mathbf{r}), \quad (\text{B.1})$$

$$\kappa\boldsymbol{\nu} \cdot \mathbf{E}_W^+(\mathbf{r}) = \boldsymbol{\nu} \cdot \mathbf{E}_W^-(\mathbf{r}), \quad (\text{B.2})$$

$$\gamma_E \kappa [\nabla \cdot \mathbf{E}_W]^+(\mathbf{r}) = [\nabla \cdot \mathbf{E}_W]^-(\mathbf{r}), \quad (\text{B.3})$$

$$\boldsymbol{\nu} \times \mathbf{H}_W^+(\mathbf{r}) = \boldsymbol{\nu} \times \mathbf{H}_W^-(\mathbf{r}), \quad (\text{B.4})$$

$$\lambda\kappa\boldsymbol{\nu} \cdot \mathbf{H}_W^+(\mathbf{r}) = \boldsymbol{\nu} \cdot \mathbf{H}_W^-(\mathbf{r}), \quad (\text{B.5})$$

$$\gamma_M [\nabla \cdot \mathbf{H}_W]^+(\mathbf{r}) = [\nabla \cdot \mathbf{H}_W]^-(\mathbf{r}). \quad (\text{B.6})$$

When (B.1) holds then also the surface divergence of (B.1) holds. By combining the surface divergence of (B.1) with (B.5) we get

$$\lambda\kappa(ik_1\boldsymbol{\nu} \cdot \mathbf{H}_2^+ + \boldsymbol{\nu} \cdot [\nabla \times \boldsymbol{\nu} \times (\boldsymbol{\nu} \times \mathbf{E}_2)]^+) = ik_1\boldsymbol{\nu} \cdot \mathbf{H}_1^- + \boldsymbol{\nu} \cdot [\nabla \times \boldsymbol{\nu} \times (\boldsymbol{\nu} \times \mathbf{E}_1)]^-, \quad (\text{B.7})$$

which by (82)–(85) and limits in Appendix A leads to

$$\begin{aligned} & \lambda\kappa \left(\kappa^{-1}\boldsymbol{\nu} \cdot [\nabla(\nabla \cdot \mathcal{S}_{k_2})]^+ (\boldsymbol{\nu}'\sigma_M + \kappa\mathbf{M}_s) - ik_1\boldsymbol{\nu} \cdot \mathcal{N}_{k_2}\varrho_M + ik_1\varrho_M \right) \\ &= -\boldsymbol{\nu} \cdot [\nabla(\nabla \cdot \mathcal{S}_{k_1})]^- (\boldsymbol{\nu}'\sigma_M + \mathbf{M}_s) + ik_1\boldsymbol{\nu} \cdot \mathcal{N}_{k_1}\varrho_M + ik_1\varrho_M. \end{aligned} \quad (\text{B.8})$$

A comparison of (B.8) with the limits $\boldsymbol{\nu} \cdot [\nabla(\nabla \cdot \mathbf{H}_1)]^-$ and $\boldsymbol{\nu} \cdot [\nabla(\nabla \cdot \mathbf{H}_2)]^+$ shows that

$$\lambda\boldsymbol{\nu} \cdot [\nabla(\nabla \cdot \mathbf{H}_2)]^+(\mathbf{r}) = \boldsymbol{\nu} \cdot [\nabla(\nabla \cdot \mathbf{H}_1)]^-(\mathbf{r}). \quad (\text{B.9})$$

Let $\psi_W = \nabla \cdot \mathbf{H}_W$, where \mathbf{H}_W is given by (95). The fundamental solution (3) and the boundary conditions (B.6) and (B.9) make ψ_W satisfy

$$\begin{cases} \Delta\psi_W(\mathbf{r}) + k_2^2\psi_W(\mathbf{r}) = 0, & \mathbf{r} \in \Omega_1, \\ \Delta\psi_W(\mathbf{r}) + k_1^2\psi_W(\mathbf{r}) = 0, & \mathbf{r} \in \Omega_2, \\ \gamma_M\psi_W^+(\mathbf{r}) = \psi_W^-(\mathbf{r}), & \mathbf{r} \in \Gamma, \\ \lambda\boldsymbol{\nu} \cdot [\nabla\psi_W]^+(\mathbf{r}) = \boldsymbol{\nu} \cdot [\nabla\psi_W]^-(\mathbf{r}), & \mathbf{r} \in \Gamma, \\ (\partial_{|\mathbf{r}|} - ik_2)\psi_W(\mathbf{r}) = o(|\mathbf{r}|^{-1}), & |\mathbf{r}| \rightarrow \infty. \end{cases} \quad (\text{B.10})$$

By rescaling ψ_W in Ω_1 , the transmission problem (B.10) is seen to be identical to problem \mathcal{B}_0 with $\alpha = \lambda\bar{\gamma}_M/|\gamma_M|^2$. It means that if $\{k_1, k_2, \alpha = \lambda\bar{\gamma}_M\}$ is such that the conditions of Section 3.3.4 hold, then (B.10) only has the trivial solution $\nabla \cdot \mathbf{H}_W(\mathbf{r}) = 0$ for $\mathbf{r} \in \Omega_1 \cup \Omega_2$.

Let $\xi_W = \nabla \cdot \mathbf{E}_W$, where \mathbf{E}_W is given by (94). From the fundamental solution (3) and the boundary conditions (B.2), (B.3), and (B.4) we can, in the same manner as above, show that ξ_W satisfies

$$\begin{cases} \Delta\xi_W(\mathbf{r}) + k_2^2\xi_W(\mathbf{r}) = 0, & \mathbf{r} \in \Omega_1, \\ \Delta\xi_W(\mathbf{r}) + k_1^2\xi_W(\mathbf{r}) = 0, & \mathbf{r} \in \Omega_2, \\ \gamma_E\kappa\xi_W^+(\mathbf{r}) = \xi_W^-(\mathbf{r}), & \mathbf{r} \in \Gamma, \\ \boldsymbol{\nu} \cdot [\nabla\xi_W]^+(\mathbf{r}) = \boldsymbol{\nu} \cdot [\nabla\xi_W]^-(\mathbf{r}), & \mathbf{r} \in \Gamma, \\ (\partial_{|\mathbf{r}|} - ik_2)\xi_W(\mathbf{r}) = o(|\mathbf{r}|^{-1}), & |\mathbf{r}| \rightarrow \infty. \end{cases} \quad (\text{B.11})$$

If the set $\{k_1, k_2, \alpha = \bar{\gamma}_E \bar{\kappa}\}$ is such that the conditions of Section 3.3.4 hold, then $\nabla \cdot \mathbf{E}_W(\mathbf{r}) = 0$ for $\mathbf{r} \in \Omega_1 \cup \Omega_2$.

We then apply the same method to \mathbf{E} and \mathbf{H} in (86) and (87). Let $\psi = \nabla \cdot \mathbf{H}$ and $\xi = \nabla \cdot \mathbf{E}$. Then

$$\begin{cases} \Delta\psi(\mathbf{r}) + k_1^2\psi(\mathbf{r}) = 0, & \mathbf{r} \in \Omega_1, \\ \Delta\psi(\mathbf{r}) + k_2^2\psi(\mathbf{r}) = 0, & \mathbf{r} \in \Omega_2, \\ \psi^+(\mathbf{r}) = \psi^-(\mathbf{r}), & \mathbf{r} \in \Gamma, \\ \kappa\boldsymbol{\nu} \cdot [\nabla\psi]^+(\mathbf{r}) = \boldsymbol{\nu} \cdot [\nabla\psi]^-(\mathbf{r}), & \mathbf{r} \in \Gamma, \\ (\partial_{|\mathbf{r}|} - ik_1)\psi(\mathbf{r}) = o(|\mathbf{r}|^{-1}), & |\mathbf{r}| \rightarrow \infty, \end{cases} \quad (\text{B.12})$$

and

$$\begin{cases} \Delta\xi(\mathbf{r}) + k_1^2\xi(\mathbf{r}) = 0, & \mathbf{r} \in \Omega_1, \\ \Delta\xi(\mathbf{r}) + k_2^2\xi(\mathbf{r}) = 0, & \mathbf{r} \in \Omega_2, \\ \xi^+(\mathbf{r}) = \kappa\xi^-(\mathbf{r}), & \mathbf{r} \in \Gamma, \\ \boldsymbol{\nu} \cdot [\nabla\xi]^+(\mathbf{r}) = \boldsymbol{\nu} \cdot [\nabla\xi]^-(\mathbf{r}), & \mathbf{r} \in \Gamma, \\ (\partial_{|\mathbf{r}|} - ik_1)\xi(\mathbf{r}) = o(|\mathbf{r}|^{-1}), & |\mathbf{r}| \rightarrow \infty. \end{cases} \quad (\text{B.13})$$

Problem (B.12) is identical to problem \mathbf{A}_0 and by rescaling ξ in Ω_2 , also problem (B.13) becomes identical to problem \mathbf{A}_0 . By that, $\nabla \cdot \mathbf{H}(\mathbf{r}) = \nabla \cdot \mathbf{E}(\mathbf{r}) = 0$ for $\mathbf{r} \in \Omega_1 \cup \Omega_2$ when $(\text{Arg}(k_1), \text{Arg}(k_2))$ is in the set of points of Figure 2(a).

C. Fulfillment of Maxwell's equations

We show that \mathbf{E} and \mathbf{H} of (86) and (87) satisfy (67)–(69) and that \mathbf{E}_W and \mathbf{H}_W of (94) and (95) satisfy (76)–(78) if $\nabla \cdot \mathbf{E}_i(\mathbf{r}) = \nabla \cdot \mathbf{H}_i(\mathbf{r}) = 0$, $i = 1, 2$, and $\mathbf{r} \in \Omega_1 \cup \Omega_2$.

The rotation of (84) and (85) are

$$\begin{aligned} \nabla \times \mathbf{H}_1(\mathbf{r}) &= \frac{ik_1}{2} \mathcal{R}_{k_1}(\boldsymbol{\nu}'\sigma_M + \mathbf{M}_s)(\mathbf{r}) + \frac{1}{2} \nabla \times \mathcal{R}_{k_1}(\boldsymbol{\nu}'\sigma_E + \mathbf{J}_s)(\mathbf{r}) \\ &\quad + \nabla \times \mathbf{H}^{\text{in}}(\mathbf{r}), \quad \mathbf{r} \in \Omega_1 \cup \Omega_2, \end{aligned} \quad (\text{C.1})$$

$$\begin{aligned} \nabla \times \mathbf{H}_2(\mathbf{r}) &= -\frac{ik_1}{2} \mathcal{R}_{k_2}(\boldsymbol{\nu}'\sigma_M + \kappa\mathbf{M}_s)(\mathbf{r}) \\ &\quad - \frac{1}{2} \nabla \times \mathcal{R}_{k_2}(\kappa^{-1}\boldsymbol{\nu}'\sigma_E + \mathbf{J}_s)(\mathbf{r}), \quad \mathbf{r} \in \Omega_1 \cup \Omega_2. \end{aligned} \quad (\text{C.2})$$

These expressions can be rewritten as

$$\begin{aligned} \nabla \times \mathbf{H}_1(\mathbf{r}) &= \frac{ik_1}{2} \mathcal{R}_{k_1}(\boldsymbol{\nu}'\sigma_M + \mathbf{M}_s)(\mathbf{r}) - \frac{ik_1}{2} \tilde{\mathcal{S}}_{k_1}(\boldsymbol{\nu}'\sigma_E + \mathbf{J}_s)(\mathbf{r}) \\ &\quad + \frac{1}{2} \nabla(\nabla \cdot \mathcal{S}_{k_1}(\boldsymbol{\nu}'\sigma_E + \mathbf{J}_s))(\mathbf{r}) + \nabla \times \mathbf{H}^{\text{in}}(\mathbf{r}), \quad \mathbf{r} \in \Omega_1 \cup \Omega_2, \end{aligned} \quad (\text{C.3})$$

$$\begin{aligned} \nabla \times \mathbf{H}_2(\mathbf{r}) &= -\frac{ik_1}{2} \mathcal{R}_{k_2}(\boldsymbol{\nu}'\sigma_M + \kappa\mathbf{M}_s)(\mathbf{r}) + \frac{ik_1}{2} \tilde{\mathcal{S}}_{k_2}(\boldsymbol{\nu}'\sigma_E + \kappa\mathbf{J}_s)(\mathbf{r}) \\ &\quad - \frac{1}{2} \nabla(\nabla \cdot \mathcal{S}_{k_2}(\kappa^{-1}\boldsymbol{\nu}'\sigma_E + \mathbf{J}_s))(\mathbf{r}), \quad \mathbf{r} \in \Omega_1 \cup \Omega_2. \end{aligned} \quad (\text{C.4})$$

If $\nabla \cdot \mathbf{E}_i = 0$, $i = 1, 2$, it follows from (82) and (83) that

$$\tilde{\mathcal{S}}_{k_1} \varrho_{\mathbf{E}}(\mathbf{r}) - \nabla \cdot \mathcal{S}_{k_1}(\boldsymbol{\nu}' \sigma_{\mathbf{E}} + \mathbf{J}_s)(\mathbf{r}) = 0, \quad \mathbf{r} \in \Omega_1 \cup \Omega_2, \quad (\text{C.5})$$

$$\tilde{\mathcal{S}}_{k_2} \varrho_{\mathbf{E}}(\mathbf{r}) - \nabla \cdot \mathcal{S}_{k_2}(\kappa^{-1} \boldsymbol{\nu}' \sigma_{\mathbf{E}} + \mathbf{J}_s)(\mathbf{r}) = 0, \quad \mathbf{r} \in \Omega_1 \cup \Omega_2. \quad (\text{C.6})$$

Then (C.3) and (C.4) can be written as

$$\begin{aligned} \nabla \times \mathbf{H}_1(\mathbf{r}) &= \frac{ik_1}{2} \mathcal{R}_{k_1}(\boldsymbol{\nu}' \sigma_{\mathbf{M}} + \mathbf{M}_s)(\mathbf{r}) - \frac{ik_1}{2} \tilde{\mathcal{S}}_{k_1}(\boldsymbol{\nu}' \sigma_{\mathbf{E}} + \mathbf{J}_s)(\mathbf{r}) \\ &\quad + \frac{ik_1}{2} \mathcal{N}_{k_1} \varrho_{\mathbf{E}}(\mathbf{r}) + \nabla \times \mathbf{H}^{\text{in}}(\mathbf{r}), \quad \mathbf{r} \in \Omega_1 \cup \Omega_2, \end{aligned} \quad (\text{C.7})$$

$$\begin{aligned} \nabla \times \mathbf{H}_2(\mathbf{r}) &= -\frac{ik_1}{2} \mathcal{R}_{k_2}(\boldsymbol{\nu}' \sigma_{\mathbf{M}} + \kappa \mathbf{M}_s)(\mathbf{r}) + \frac{ik_1}{2} \tilde{\mathcal{S}}_{k_2}(\boldsymbol{\nu}' \sigma_{\mathbf{E}} + \kappa \mathbf{J}_s)(\mathbf{r}) \\ &\quad - \frac{ik_1}{2} \mathcal{N}_{k_2} \varrho_{\mathbf{E}}(\mathbf{r}), \quad \mathbf{r} \in \Omega_1 \cup \Omega_2. \end{aligned} \quad (\text{C.8})$$

The Ampère law

$$\nabla \times \mathbf{H}_1(\mathbf{r}) = -ik_1 \mathbf{E}_1(\mathbf{r}), \quad \mathbf{r} \in \Omega_1 \cup \Omega_2, \quad (\text{C.9})$$

$$\nabla \times \mathbf{H}_2(\mathbf{r}) = -ik_1 \kappa \mathbf{E}_2(\mathbf{r}), \quad \mathbf{r} \in \Omega_1 \cup \Omega_2. \quad (\text{C.10})$$

now follows by combining (C.7) with (82), and (C.8) with (83).

The Faraday law

$$\nabla \times \mathbf{E}_1(\mathbf{r}) = ik_1 \mathbf{H}_1(\mathbf{r}), \quad \mathbf{r} \in \Omega_1 \cup \Omega_2, \quad (\text{C.11})$$

$$\nabla \times \mathbf{E}_2(\mathbf{r}) = ik_1 \mathbf{H}_2(\mathbf{r}), \quad \mathbf{r} \in \Omega_1 \cup \Omega_2, \quad (\text{C.12})$$

follows in the same manner from $\nabla \cdot \mathbf{H}_i = 0$, $i = 1, 2$, and by combining the rotation of (82) with (84) and the rotation of (83) with (85).

From (C.9)–(C.12) it follows that \mathbf{E} and \mathbf{H} of (86) and (87) satisfy (67)–(69) and that \mathbf{E}_W and \mathbf{H}_W of (94) and (95) satisfy (76)–(78).

D. Uniqueness for problems C, C₀, and D₀

We sketch a proof that problem C₀ has only the trivial solution and that problem C has at most one solution by relating these problems to problem A₀ and A. We also show that the criteria for problem D₀ to only have the trivial solution are the same as the criteria in Section 3.3.4 that make problem B₀ only have the trivial solution.

Let S_R be a sphere of radius R with outward unit normal \mathbf{n} . Assume that S_R is sufficiently large to contain Γ and let $\Omega_{1,R} = \{\mathbf{r} \in \Omega_1 : |\mathbf{r}| < R\}$. From Gauss' theorem and Section 3.1 we obtain an energy relation for problem A₀

$$\int_{S_R} (U \nabla \bar{U}) \cdot \mathbf{n} \, dS = \int_{\Omega_{1,R}} (|\nabla U|^2 - \bar{k}_1^2 |U|^2) \, dv + \int_{\Omega_2} (\bar{\kappa}^{-1} |\nabla U|^2 - \bar{k}_1^2 |U|^2) \, dv. \quad (\text{D.1})$$

The corresponding relation for problem C_0 in Section 8.1 is

$$\begin{aligned} -i\bar{k}_1 \int_{S_R} (\bar{\mathbf{E}} \times \mathbf{H}) \cdot \mathbf{n} \, dS &= \int_{\Omega_{1,R}} (|k_1|^2 |\mathbf{E}|^2 - \bar{k}_1^2 |\mathbf{H}|^2) \, dv \\ &+ \int_{\Omega_2} (|k_1 \kappa|^2 \bar{\kappa}^{-1} |\mathbf{E}|^2 - \bar{k}_1^2 |\mathbf{H}|^2) \, dv. \end{aligned} \quad (D.2)$$

The right hand sides of (D.1) and (D.2) are equivalent. By using techniques similar to those in [15, pp. 309–310] and [16, p. 1434], it is then quite straightforward to show that when $(\text{Arg}(k_1), \text{Arg}(k_2))$ is in the set of points of Figure 2(a), then $U = 0$ and $\mathbf{E} = \mathbf{H} = \mathbf{0}$ for $\mathbf{r} \in \Omega_1 \cup \Omega_2$. Standard arguments give that problem C has at most one solution when problem C_0 only has the trivial solution.

From Section 3.2 we obtain an energy relation for problem B_0

$$\begin{aligned} \int_{S_R} (W \nabla \bar{W}) \cdot \mathbf{n} \, dS &= \int_{\Omega_{1,R}} (|\nabla W|^2 - \bar{k}_2^2 |W|^2) \, dv \\ &+ \bar{\alpha}^{-1} \int_{\Omega_2} (|\nabla W|^2 - \bar{k}_1^2 |W|^2) \, dv. \end{aligned} \quad (D.3)$$

The corresponding relation for problem D_0 in Section 8.2 is

$$\begin{aligned} -i\bar{k}_1 \bar{\kappa} \int_{S_R} (\bar{\mathbf{E}}_W \times \mathbf{H}_W) \cdot \mathbf{n} \, dS &= \int_{\Omega_{1,R}} (|k_1 \kappa|^2 |\mathbf{E}_W|^2 - \bar{k}_2^2 |\mathbf{H}_W|^2) \, dv \\ &+ \bar{\lambda}^{-1} \int_{\Omega_2} (|k_1|^2 |\mathbf{E}_W|^2 - \bar{k}_1^2 |\mathbf{H}_W|^2) \, dv. \end{aligned} \quad (D.4)$$

The right hand sides of (D.3) and (D.4) are equivalent and we can again use results from [15, pp. 309–310] and [16, p. 1434] to find the criteria that lead to $W = 0$ and $\mathbf{H}_W = \mathbf{E}_W = \mathbf{0}$. These are the criteria for the set $\{k_1, k_2, \alpha = \lambda\}$ in Section 3.3.4.

References

- [1] A. Axelsson, “Transmission problems for Maxwell’s j equations with weakly Lipschitz interfaces”, *Math. Methods Appl. Sci.*, **29**, 665–714 (2006).
- [2] A.-S. Bonnet-Ben Dhia and C. Carvalho and L. Chesnel and P. Ciarlet, “On the use of perfectly matched layers at corners for scattering problems with sign-changing coefficients”, *J. Comput. Phys.*, **322**, 224–247 (2016).
- [3] D. Colton and R. Kress, *Integral equation methods in scattering theory*, John Wiley & Sons Inc., New York, 1983.
- [4] D. Colton and R. Kress, *Inverse acoustic and electromagnetic scattering theory*, 2nd ed., *Appl. Math. Sci.*, vol. 93, Springer-Verlag, Berlin, 1998.

- [5] C. L. Epstein, L. Greengard, and M. O’Neil, “Debye sources and the numerical solution of the time harmonic Maxwell equations II”, *Comm. Pure Appl. Math.*, **66**, 753–789 (2013).
- [6] C. L. Epstein, L. Greengard, and M. O’Neil, “A high-order wideband direct solver for electromagnetic scattering from bodies of revolution”, *J. Comput. Phys.*, **387**, 205–229 (2019).
- [7] J. Helsing, “Integral equation methods for elliptic problems with boundary conditions of mixed type”, *J. Comput. Phys.*, **228**, 8892–8907 (2009).
- [8] J. Helsing, “Solving integral equations on piecewise smooth boundaries using the RCIP method: a tutorial”, *arXiv:1207.6737v9 [physics.comp-ph]* (revised 2018).
- [9] J. Helsing and A. Karlsson, “Resonances in axially symmetric dielectric objects,” *IEEE Trans. Microw. Theory Tech.*, **65**, 2214–2227 (2017).
- [10] J. Helsing and A. Karlsson, “On a Helmholtz transmission problem in planar domains with corners,” *J. Comput. Phys.*, **371**, 315–332 (2018).
- [11] J. Helsing and A. Karlsson, “Physical-density integral equation methods for scattering from multi-dielectric cylinders,” *J. Comput. Phys.*, **387**, 14–29 (2019).
- [12] J. Helsing and K.-M. Perfekt, “The spectra of harmonic layer potential operators on domains with rotationally symmetric conical points”, *J. Math. Pures Appl.*, **118**, 235–287 (2018).
- [13] J. Homola, “Surface plasmon resonance sensors for detection of chemical and biological species”, *Chem. Rev.*, **108**, 462–493 (2008).
- [14] A. Kirsch and F. Hettlich, *The mathematical theory of time-harmonic Maxwell’s equations*, *Appl. Math. Sci.*, vol. 190, Springer, Cham, 2015.
- [15] R.E. Kleinman and P.A. Martin, “On single integral equations for the transmission problem of acoustics”, *SIAM J. Appl. Math.*, **48**, 307–325 (1988).
- [16] R. Kress and G.F. Roach. “Transmission problems for the Helmholtz equation”, *J. Math. Phys.*, **19**, 1433–1437 (1978).
- [17] G. Kristensson, *Scattering of electromagnetic waves by obstacles*, Mario Boella Series on Electromagnetism in Information and Communication, SciTech Publishing, Edison, NJ, 2016.
- [18] J. Lai and M. O’Neil, “An FFT-accelerated direct solver for electromagnetic scattering from penetrable axisymmetric objects”, *J. Comput. Phys.*, **390**, 152–174 (2019).
- [19] J. Li, F. Xi, and B. Shanker, “Decoupled potential integral equations for electromagnetic scattering from dielectric objects”, *IEEE Trans. Antennas Propag.*, **67**, 1729–1739 (2018).
- [20] X. Luo, D Tsai, M Gu, and M Hong, “Extraordinary optical fields in nanostructures: from sub-diffraction-limited optics to sensing and energy conversion” *Chem. Soc. Rev.*, **48**, 2458–2494 (2019).

- [21] J.R. Mautz and R.F. Harrington. “Electromagnetic scattering from a homogeneous body of revolution”, Tech. Rep. TR-77-10, Dept. of electrical and computer engineering, Syracuse Univ., New York, (1977).
- [22] C. Müller, *Foundations of the Mathematical Theory of Electromagnetic Waves*. Berlin, Springer-Verlag, 1969.
- [23] H. Raether, *Surface plasmons on smooth and rough surfaces and on gratings*, vol. 111 of *Springer tracts in modern physics*, Springer, Berlin, 1988.
- [24] M. Taskinen and P. Ylä-Oijala, “Current and charge integral equation formulation”, *IEEE Trans. Antennas Propag.*, **54**, 58–67 (2006).
- [25] D. Tzarouchis and A. Sihvola, “Light scattering by a dielectric sphere: perspectives on the Mie resonances”, *Appl. Sci.*, **8**, 184–205 (2018).
- [26] F. Vico, Z. Gimbutas, L. Greengard, and M. Ferrando-Bataller, “Overcoming low-frequency breakdown of the magnetic field integral equation”, *IEEE Trans. Antennas Propag.*, **61**, 1285–1290 (2013).
- [27] F. Vico, M. Ferrando-Bataller, T. Jiménez, and D. Sánchez-Escuderos, “A non-resonant single source augmented integral equation for the scattering problem of homogeneous lossless dielectrics”, 2016 IEEE Int. Symp. Antennas Propag. (APSURSI), 745–746 (2016).
- [28] F. Vico, L. Greengard, and M. Ferrando. “Decoupled field integral equations for electromagnetic scattering from homogeneous penetrable obstacles”, *Comm. Part. Differ. Equat.* **43**, 159–184 (2018).
- [29] P. Young, S. Hao, and P.G. Martinsson, “A high-order Nyström discretization scheme for boundary integral equations defined on rotationally symmetric surfaces”, *J. Comput. Phys.*, **231**, 4142–4159 (2012).